Combinatorics of triangulations

March 2001

by

Fumihiko Takeuchi

A Dissertation

Submitted to

The Graduate School of Information Science
The University of Tokyo
in Partial Fulfillment of the Requirements
for the Degree for Doctor of Science

Thesis Supervisor: Hiroshi Imai
Title: Associate Professor of Information Science

ABSTRACT

Several combinatorial aspects of triangulations and their generalizations are studied in this thesis. A triangulation of a point configuration and a d-dimensional polyhedron whose vertices are among the points is a decomposition of the polyhedron using d-simplices with vertices among the points.

The two main fields triangulations appear are combinatorial geometry in mathematics and computational geometry in information science. The topics connected to triangulations in combinatorial geometry include, polytope theory, Gröbner bases of affine toric ideals, Hilbert bases, generalized hypergeometric functions, and Ehrhart polynomials. Many fields of computational geometry, such as computer graphics, solid modeling, mesh generation, and motion planning, use triangulations extensively. The problems we consider are among the main interests in combinatorial geometry. The topics are on simplified basic situations for computational geometry, but are those arising in applications and giving advice for planning algorithms.

The objects we study are those around triangulations: (1) triangulations and dissections of 3-polytopes, (2) triangulations (mainly) in the plane, (3) 2-dimensional spheres, and (4) 2-dimensional simplicial complexes. They are from rigid to abstract in this order. The properties of these objects we are interested in are (1) sizes, (2) regularity, which represents the convexity of triangulations, (3) geometric shellings, which are combinatorial topological properties but still expressing convexity, and (4) shellability, extendable shellability, vertex decomposability, which are combinatorial topological properties on incremental construction. They are from basic to fine in this order. The properties become difficult to understand as the dimension becomes higher. We studied the most fundamental cases: basic properties for rigid objects, and fine properties for abstract objects. Four results among our studies are introduced. (See Chapter 1 for the sketch of this thesis.)

The first one is on sizes of decompositions. Dissections are decompositions in which simplices are not required to intersect nicely to form simplicial complexes. They make a superclass of triangulations. We showed size difference between these two kinds of decompositions for 3-polytopes. We also gave bounds for the size of dissections of 3-polytopes which are similar to the bounds known for triangulations. (Chapter 2)

The second result is on nonregular triangulations. We defined a graph representing the in_front/behind order of the maximal dimensional simplices in a triangulation when viewed from a point. The triangulations having some asymmetric cycle in this graph forms a subclass of nonregular triangulations. Thus, we gave a combinatorial subclass of nonregular triangulations, which is of interest, and also studied them further exploiting linear programming duality. (Chapter 3)

The third result is on combinatorial topological properties. Here, we studied geometric shellings, shellings becoming line shellings in some combinatorially equivalent polytopes, of 3-polytopes. We showed several sufficient conditions for a shelling to be a geometric shelling, which are of interest both in polytope and graph theory. (Chapter 4)

The last result also is on combinatorial topological properties. The subject here is the difference between incremental construction properties, namely, shellability, extendable shellability, and vertex decomposability. By enumerating shellable nonpseudomanifolds of small size, we found smallest examples showing the difference of these classes, and examples uncovering a relation which was not known. (Chapter 5)

An approach in this thesis was to use computers to generate and test examples to study combinatorial geometric aspects of triangulations. We not only devised algorithms of our own, but also made use of established techniques such as integer programming and convex hull computation. (Chapter 6)

Acknowledgments

I would like to thank Hiroshi Imai, Masahiro Hachimori, David Bremner, Ken'ichi Asai, Seiko Minami, other members of Imai laboratory and Akiko Shintani. My deep acknowledgments are to Jesús A. De Loera, Takayuki Ishizeki, Sonoko Moriyama and Francisco Santos, for the great experience working together and their kindness to allow the resulting jointworks to be included in this thesis.

For Chapter 2, I am grateful to Jesús A. De Loera and Francisco Santos with whom this chapter was worked. Thanks to Alexander Below and Jürgen Richter-Gebert for their help and ideas in the proofs of Proposition 2.7 and 2.9, Alexander Below for making Figure 2.9 using the package Cinderella, Akira Tajima and Jörg Rambau for corroborating many of the computational results, Samuel Peterson for his help with calculations, and Hiroshi Imai, Bernd Sturmfels and Akira Tajima for their support.

For Chapter 3, thanks to Kenji Kashiwabara for bringing the problem to the author's interest, and Hervé Brönnimann, Masahiro Hachimori, Hiroshi Imai, Mary Inaba, Francisco Santos, Akihisa Tamura and an anonymous referee for comments and encouragements.

For Chapter 4, I am grateful to Takayuki Ishizeki with whom this chapter was worked. Thanks to David Avis, Jesús A. De Loera, Masahiro Hachimori, Ryuichi Hirabayashi, Yoshiko Ikebe, Hiroshi Imai and Shin-ichi Tokunaga for discussions, comments and information.

For Chapter 5, I am grateful to Sonoko Moriyama with whom this chapter was worked. Thanks to David Avis, Hiroshi Imai and especially Masahiro Hachimori for discussions and encouragements.

Finally, cordial acknowledgments are to my family and my friends for their support during the years of my graduate study.

Table of Contents

Chapter 1

Triangulations, their generalizations and applications

The main results of this thesis are sketched in this section. The mathematical details are discussed in Chapters 2 to 5. Here, we emphasize on applications leading to the problems we discuss. Our results might give suggestions on designing algorithms for these applications.

Each section introduces one object from triangulations and their generalizations. We discuss their applications and properties of interest, though restricting mainly to those subjects relevant to our results. See Figure 1.1.

Properties become substantially difficult when the dimension is raised. In each dimension, we analyze fundamental problems: basic properties for rigid objects and fine properties for abstract objects. For basic terminology, see [46] [106].
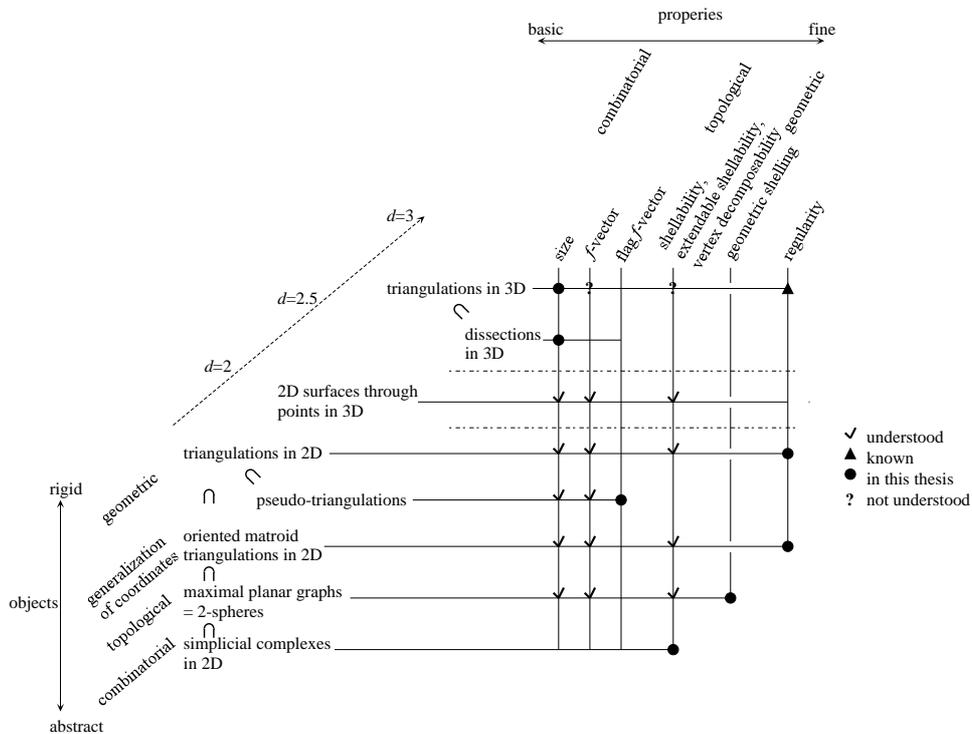
Figure 1.1: Triangulations, their generalizations and their properties.

1.1 Triangulations

1.1.1 Definitions and examples

Definition 1.1. *Given points $p_1, \ldots, p_n \in \mathbb{R}^d$ and a d-dimensional (possibly nonconvex) polyhedron including these points and with vertices among the points, a set of d-simplices with vertices among these points is a* triangulation *if (1) any pair of d-simplices intersect at their (possibly empty) face, and (2) the union of the d-simplices is equal to the polyhedron.*

The representation of a polyhedron needs some arguments, but we skip them here. In some situations (often in computational geometry) we are forced to use all the given points in the triangulation, and in some other situations (often in combinatorial geometry) we are not. As an example, all of the five triangulations of a pentagon with its vertices the point configuration is given in Figure 1.2.
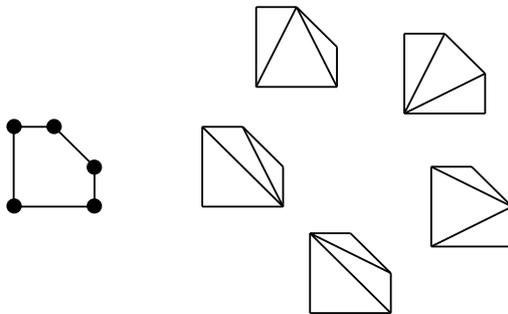
Figure 1.2: Triangulations of a pentagon.

1.1.2 Applications

Triangulations in 2D

Triangulations in dimension two give partitions of the given polygon, and are fundamental in computational geometry [35] [46, Chapter 22]. Among important applications are Geometric Information Systems or image processing. Extensive work has been done in this field. The Delaunay triangulation for a given point configuration is known to possess various nice properties such as maximizing the minimum angle. All triangulations of a given point configurations can be transformed to each other by sequences of local changes called *flips*, which is convenient when optimizing triangulations.

Triangulations in 3D

Triangulations in dimension three are also important, because objects surrounding us are of this dimension. For example, mesh generation or Computer Aided Design are important applications of triangulations.

Compared to dimension two, the case dimension three (or more) becomes much more complicated, and a number of fundamental questions are still remaining unsolved. Let us list a few facts:

- The number of triangles in triangulations in dimension two using all of the given points is determined uniquely by the point configuration, however, there are cases the number of tetrahedra in triangulations in dimension three vary for different triangulations even for the same point configuration and the polyhedron.
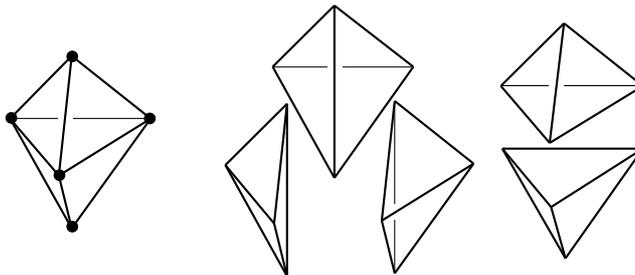
Figure 1.3: Triangulations into three or two tetrahedra.

- There exists a nonconvex polyhedron, for example, Schönhardt's polyhedron, which does not have a triangulation (if points other than the vertices of the polyhedron cannot be used) [46, Section 22.5]. Furthermore, deciding whether a given three dimensional (nonconvex) polyhedron has a triangulation or not is NP-complete [85].

- Computing the minimal number of tetrahedra required in a triangulation of a 3-dimensional (convex) polytope is NP-complete [6].

- It is not known whether all triangulations for a given point configuration and its convex hull can be transformed to each other by sequences of flips, for the case $d = 3, 4, 5$. As mentioned above, it is true for $d = 2$. It is known to be false for $d = 6$ [86].

1.1.3 Properties and questions

Size and complexity

By the *size* of a triangulation, we mean the number of d-simplices in it. As indicated above, the size of triangulations in three or higher dimensions varies even for the same given set of points and polyhedron. Thus, this size becomes a matter of question.

Computationally, it is important to keep this size small. The *adjacency graph* of a triangulation is a graph with its vertices corresponding to the d-simplices in the triangulation and edges between pairs of vertices corresponding to d-simplices sharing their facets. Finding a triangulation whose size of this adjacency graph is small is also important.

Triangulations in 2D using all the given points have constant size. Also, their applications often involve large number of points. Thus, it becomes important to care not merely the size but

more finer properties as complexity. Pseudo-triangulations (see Section A.1) are generalizations of triangulations in 2D for such purpose.

In_front/behind view ordering of simplices

In computer graphics, understanding the in_front/behind order of the simplices in a triangulation viewed from a specific point, as in the figure below, is fundamental [36].
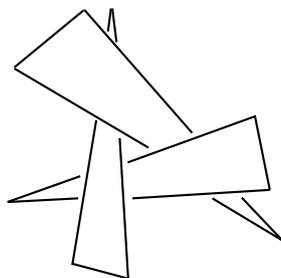
Figure 1.4: Cyclic in_front/behind order of triangles viewed from a point.

Orderings for incremental construction

Orderings of d-simplices (or vertices) for incremental construction is important in the following areas. The time and space complexity of computations in such applications depend on the ordering of the d-simplices the computation is based on.

(1) The ordering is important in constructing the triangulation, or in computing some function on the triangulated polyhedron as in mesh generation. In these cases, the coordinates of the points in the triangulation are required.

(2) The ordering is important also in analyzing the morphology of the polyhedron. In this case, the information only on the connection of the d-simplices (i.e. the information on the underlying simplicial complex, see Section 1.5) might be sufficient.

Regularity

A triangulation of a d-dimensional convex polytope is *regular* if it can appear as the projection of the lower faces of the boundary complex of a $(d + 1)$-dimensional convex polytope. The condition of regularity means the "convexity" of the triangulation. For example, when a triangulation is regular, we can find line shellings [18], special kinds of nice orderings of d-simplices for incremental construction. The definition of regularity can be extended to nonconvex polyhedra: a triangulation (of a nonconvex polyhedron) is regular if it forms a subset of some regular triangulation of a convex polytope. An example of a nonregular triangulation is given below.

Regular triangulations altogether for a point configuration (and its convex hull) are forming a polytopal structure described by the secondary polytope [44] [45]. This result implies that all regular triangulations for a given point configuration can be transformed to each other by sequences

4
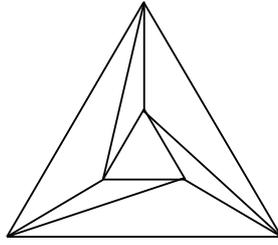
Figure 1.5: A nonregular triangulation.

of flips. In connection with Gröbner bases, initial ideals for the affine toric ideal determined by a point configuration correspond to the regular triangulations of the point configuration [99] [100]. Regular triangulations are a generalization of the Delaunay triangulation well known in computational geometry [35], and have also been used in this field too. Since regular triangulations are connected by flips, we can perform optimization on triangulations by updating triangulations locally by flips. Also, the regularity guarantees shellability enabling incremental construction of the whole triangulation.

On the other hand, nonregular triangulations, known to be behaving differently from regular triangulations, are not yet well understood. For example, the counterexample in $d = 6$ against all triangulations being transformable by sequences of flips is a nonregular triangulation with no flips [86].

1.1.4 Our contribution

The most basic case of triangulations in dimension three are the triangulations of 3-dimensional convex polytopes. Even for this case the size of triangulations are of questions. Also, finding minimal (and maximal too probably) triangulations for 3-polytopes in general is computationally intractable. We analyze minimal and maximal size triangulations for specific non-simplicial 3-polytopes of interest: prisms, antiprisms, Archimedean solids, and combinatorial d-cubes (Theorem 2.2).

Nonregular triangulations are not understood well. We aim to put some insight into these nonregular triangulations. The connection between nonregularity and the in-front/behind view ordering was first investigated in [36]. We introduce a different in-front/behind view ordering, restricted to d-simplices in the triangulation, which agrees better with the combinatorial structure of triangulations such as adjacency graphs. We prove that triangulations having a cycle the reverse of which is not a cycle in this in-front/behind order viewed from some point are forming a (proper) subclass of nonregular triangulations. We use linear programming duality to investigate further properties of nonregular triangulations in connection with this graph (Theorem 3.1).

5

1.2 Dissections

1.2.1 Definitions and examples

Definition 1.2. *Given points $p_1, \ldots, p_n \in \mathbb{R}^d$ and a d-dimensional (possibly nonconvex) polyhedron including these points and with vertices among the points, a set of d-simplices with vertices among these points is a* dissection *if* (1) *any pair of d-simplices have no interior point in common, and* (2) *the union of the d-simplices is equal to the polyhedron.*

The representation of a polyhedron needs some arguments, but we skip them here. Dissections form a superclass of triangulations. For points in general position (i.e. no $d + 1$ points included in a hyperplane), these two classes become equal. Examples are shown in Figure 1.6.
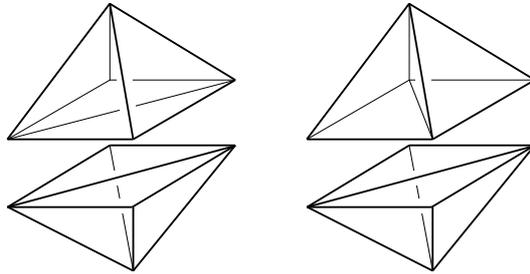
Figure 1.6: Dissections of an octahedron. Only the left one is a triangulation.

Dissections are same as triangulations in that they partition the given polyhedron, but are different in that they do not form simplicial complexes (see Section 1.5).

1.2.2 Applications

Volume computation

Computing the volume of a polyhedron is a basic operation in handling concrete objects [48]. Also, in some problems, the constraints of the problem define a polyhedron, and the number of the solutions becomes the volume of the polyhedron [97]. Volume computation becomes important also in such cases. (See Section 1.2.3 below for using dissections for volume computation.)

Hilbert bases

Dissections are related to the study of Hilbert bases and the hierarchy of covering properties for polyhedral cones, which are relevant to algebraic geometry and integer programming (see [19] [41] [89]).

Simplexity of the cube

The regular d-dimensional cube has been widely studied for its smallest dissections [24, Section C9] [52] [55]. This receives the name of *simplexity* of the cube. This was motivated by the study

6

on fixed points. Since dissections include triangulations, there is chance a minimal dissection is smaller than a minimal triangulation.

1.2.3 Properties and questions

Size

By the *size* of a dissection, we mean the number of d-simplices in it.

Since dissections, different from triangulations, do not form simplicial complexes, they become less useful in computing or analyzing some information on the whole polyhedron. However, they are useful enough in certain applications like volume computation. In such applications, it often happens to be important to keep the size of the dissection small.

If there are dissections significantly smaller than triangulations, dissections become more useful, compensating the drawback of not forming simplicial complexes. Thus, the difference of sizes between dissections and triangulations becomes one of the main questions. Little has been known on this difference. One thing known is the existence of 3-polytopes with size gap between minimal dissections and minimal triangulations [5].

1.2.4 Our contribution

The first fundamental and interesting case to study the difference between dissections and triangulations is the case of 3-polytopes. Our results are as follows:

- The gap between the size of a maximal dissection and a maximal triangulation can grow linearly on the number of vertices, and this occurs already for a family of simplicial convex 3-polytopes (Corollary 2.4).

- There is a 3-polytope in which, simultaneously, the size of a minimal (maximal) dissection is smaller (larger) than any minimal (maximal) triangulation (Proposition 2.5).

- We study how the *mismatching regions*, the polygonal mismatching parts of facets of tetrahedra, of dissections of 3-polytopes look like (Lemma 2.6).

- We prove lower and upper bounds on the size of dissections of 3-polytopes with respect to the number of vertices (Proposition 2.7). Our proof relates the f-vector of a dissection with that of some 3-ball.

1.3 2D surfaces through points in 3D

1.3.1 Definitions

Definition 1.3. *Given points $p_1, \ldots, p_n \in \mathbb{R}^3$, a set of triangles with vertices among these points is a 2-dimensional surface if (1) any pair of triangles intersect at their (possibly empty) face, and (2) the union of triangles including any vertex is homeomorphic to a 2-dimensional disc.*

1.3.2 Applications

Model representation

Representing the boundary of a 3-dimensional object as a surface is fundamental in computer graphics and solid modeling [20] [32, Section I.4]. The above definition of surfaces can directly be extended to allow not only triangles but also squares or convex polygons, which appear in such applications. Nice data structure for modeling, or the ordering of the components benefits fast rendering, compression [56], etc.

Feature extraction

After representing a 3-dimensional object by a surface, it becomes important to analyze the shape of the object [32, Section I.4]. Questions to be asked are the number of connected components, tunnels, voids, pockets, etc. These are important also in molecular modeling [37].

3D surfaces in 4D space

A situation in one dimension higher, triangulated 3-dimensional surface in 4-dimensional space, also have applications. For example, partitioning the 3-dimensional space with one more dimensional of data (such as, temperature, pressure) leads to this problem. In this situation, rather than recognizing the whole shape, queries on the data as a database might become of interest [62].

1.3.3 Properties and questions

Orderings for incremental construction

Nice orderings of triangles (or vertices) are important for manipulating surfaces. The time and space complexity of such computations depend on the ordering of the triangles the computation is based on. Applications can be classified by the data needed for computation.

(1) The ordering is important in constructing, rendering, compressing, and some topics of feature extracting. In these cases, the coordinates of the points in the surface are required.

(2) The ordering is important also in extracting topological features [30]. In this case, the information only on the connection of the triangles (i.e. the information on the underlying simplicial complex, see Section 1.5) is sufficient.

We handle those of type (2).

1.3.4 Our contribution

A 2-dimensional surface in 3-dimensional space has the structure of an abstract 2-dimensional simplicial complex underlying it (forgetting the coordinates of the points). This level of simplicial complexes has enough information to analyze the orderings of triangles (or vertices) for constructing the surface incrementally. We study such orderings for simplicial complexes (see Section 1.5.4).

1.4 Balls, spheres

1.4.1 Definitions and examples

Balls and spheres are objects of topological level. A triangulation, a surface, or an oriented matroid triangulation has a topological structure underlying it. In this (combinatorial) topological level, we forget the coordinates of the points, but keep information on the "shape" of the object expressed by how the components (e.g. d-simplices) are connected.

Definition 1.4. *Let V be a finite set. A collection Δ of subsets of V is a* simplicial complex *on V, if $\sigma \in \Delta$, $\tau \subset \sigma$ implies $\tau \in \Delta$. We call Δ a d-ball (resp. a d-sphere) if the geometric realization (i.e. the union of the convex hull of the subsets in Δ, after embedding the vertices in V in a sufficiently high dimensional space) is homeomorphic to the standard d-dimensional ball (resp. standard d-dimensional sphere).*

For example, for $V = \{1, 2, 3, 4\}$,

$$\Delta = \{123, 124, 134, 234, 12, 13, 14, 23, 24, 34, 1, 2, 3, 4, \emptyset\}$$

is a simplicial complex on V. As for notation, for example, 123 denotes $\{1, 2, 3\}$. It appears as the boundary of a tetrahedra, and is a 2-sphere.

1.4.2 Applications

Undirected graphs of polytopes

The (*undirected*) *graph of a polytope* is a graph with the vertices corresponding to the vertices of the polytope, and edges between vertices connected by an edge in the polytope. Steinitz' theorem says that an (undirected) graph is a graph of a 3-polytope if and only if it is simple, planar and 3-connected (see [106]). Furthermore, the face lattice of a 3-polytope is determined uniquely by the graph. Any 2-sphere corresponds to a maximal planar graph and to a simplicial 3-polytope. (All 3-polytopes can be covered if we extend the definition of 2-spheres to allow not only triangular but also polygonal faces.) Studies on 4-polytopes have been done recently [83], but it seems difficult to extend Steinitz' theorem to 4-polytopes [106].

Directed graphs of polytopes

A polytope and a (generic) vector in its space, define a directed graph. The underlying graph is the graph of the polytope, but we direct the edges from a vertex with smaller inner product with the vector to the vertex with larger inner product. Such kind of a graph is called a *directed graph of a polytope*. This graph is important in linear programming, especially for simplex methods. The characterization of directed graphs of 3-polytopes in graph theoretical terms has been done recently [53][74].

The vector also defines a total order on the vertices of the polytope by sorting according to the inner product with the vector (or sweeping along this direction). A total order of vertices of a polytope which can appear like this for some combinatorially equivalent polytope and some vector

is called a *polar geometric shelling*. This total order has strong connection with abstract linear programming [43], a generalization of linear programming. Examples of polytopes with some total order of vertices satisfying a weaker condition of *polar shelling*, but not of the polar geometric shelling are known [50] [93].

Directed graphs or total orders of vertices for 2-spheres correspond to the special case of simplicial 3-polytopes.

Polytopality

As mentioned above, a 2-sphere always appears as the boundary of some simplicial 3-polytope. However, 3-spheres do not necessarily appear as boundaries of 4-polytopes. Recently, *polytopality*, the measurement how close a 3-sphere is to a boundary of a polytope, has been studied [63]. For a sphere, appearing as a boundary of a polytope means convexity, and has relation with regularity discussed in Section 1.1.3.

1.4.3 Properties and questions

Polar (geometric) shellings of 3-polytopes

As mentioned above, the characterization of directed graphs of 3-polytopes has been done recently [53][74]. It would be interesting to study more concrete examples here. Also, characterizing polar shelling and understanding the difference between polar shelling and polar geometric shelling must be of interest.

1.4.4 Our contribution

For total orders of vertices of a graph of a 3-polytope, we characterize the weaker condition of being a polar shelling in graph theoretical terms (Theorem 4.2). We also give some sufficient conditions for polar geometric shellings, which might be of interest in polytope theory (Theorem 4.4). We also show the example of a 3-polytope with smallest number of vertices having a polar shelling which is not a polar geometric shelling (Example 4.7).

1.5 Simplicial complexes

1.5.1 Definitions and examples

A simplicial complex is a combinatorial structure underlying a triangulation, a surface, an oriented matroid triangulation, a ball, or a sphere. In this combinatorial level, we forget the coordinates of the points, or the topological restriction of the whole object, and in the most abstract level, only observe the information how the components are connected.

Definition 1.5. *Let V be a finite set. A collection Δ of subsets of V is a* simplicial complex on V, *if $\sigma \in \Delta$, $\tau \subset \sigma$ implies $\tau \in \Delta$.*

See Section 1.4.1 for an example.

1.5.2 Applications

In computational geometry

Simplicial complexes are of fundamental level, and appear, even unnoticed, in various scenes in computational geometry such as (Delaunay) triangulations [35], or α-shapes [38]. Considering simplicial complexes in general might be too broad, but focusing on this level, keeping the restriction of the original setting might lead to fruitful results in computational geometry.

In combinatorics

Simplicial complexes are fundamental in combinatorial geometry and in algebra. The Stanley-Reisner ring, a ring defined for a simplicial complex, bridges between these two fields [97]. The upper bound theorem bounding the number of faces of a sphere [95], and the g-theorem characterizing the face number of simplicial polytopes [8] [9] [96] were accomplished through this approach.

1.5.3 Properties and questions

Orderings for incremental construction

In computational geometry, nice orderings for incremental construction of triangulations or surfaces are important for rendering, compression, feature extraction, etc. Nice orderings for such applications can be studied in the most fundamental level of simplicial complexes.

In combinatorics, nice properties for incremental construction of simplicial complexes often have nice counterparts in the algebra side. For example, shellability implies Cohen-Macaulayness [97], or has an equivalent counterpart in algebra [34] [92].

Hierarchy of incremental construction properties has been defined and applications of such properties in other fields have been studied. However, some basic questions such as the difference between these properties, or how minimal examples look like are not answered yet. Thus, studying small concrete examples is important.

1.5.4 Our contribution

We consider three properties describing how nicely a simplicial complex can be constructed incrementally. *Shellability* means there is a nice ordering of d-simplices to construct the whole simplicial complex by pasting d-simplices one by one. *Extendable shellability* is a stronger property requiring that we do not get stuck during this process of pasting d-simplices. *Vertex decomposability* means that we can construct the whole simplicial complex by adding vertices one by one. When adding a vertex, we might be able to add more than one new d-simplices. Extendable shellability or vertex decomposability implies shellability.

We study minimal examples (in dimension two) showing the difference of these classes:

- We found minimal examples of shellable but not extendably shellable simplicial complexes, which are smaller than those previously known (Theorem 5.1).

- We also give new examples of shellable but not vertex decomposable simplicial complexes (Theorem 5.2).

- An extendably shellable but not vertex decomposable example is also shown. This indicate that neither extendable shellability nor vertex decomposability implies the other (Corollary 5.3).

- Some analysis on such minimal examples is also given (Proposition 5.14).

- We also give a rather efficient algorithm for enumerating these objects (Algorithm 5.20, Theorem 5.21).

1.6 Overview

The objects we analyze in this thesis are triangulations and their generalizations. We are interested in three kinds of their properties:

- size and complexity (Chapter 2),

- regularity and view graph (Chapter 3), and

- total order for incremental construction (Chapters 4, 5).
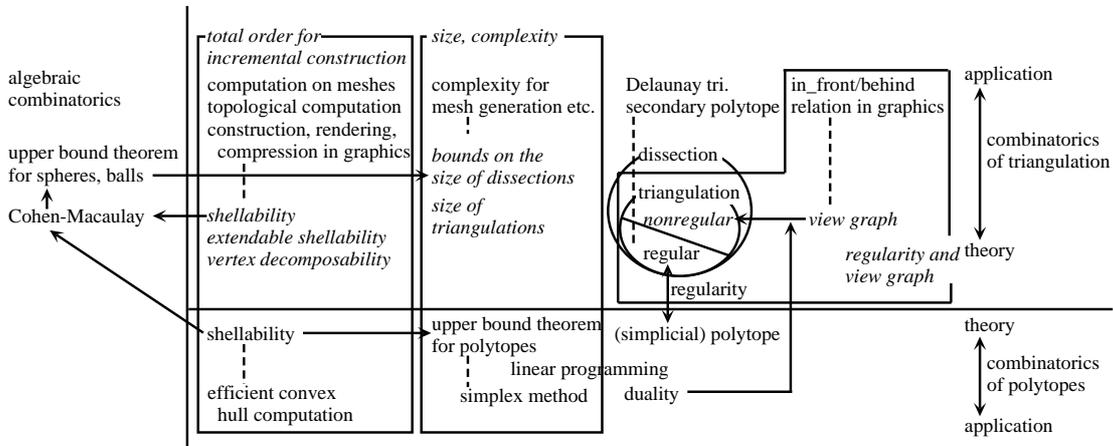
Figure 1.7: Overview of our main results

Size and complexity are the most fundamental combinatorial properties. Once we understand the size, the number of components, our next interest becomes the relations between the components. Among such relations, we focus on *total orders for incremental construction*. Analysis on such total orders are important, because they lead to results on size and complexity by providing frameworks for mathematical inductions.

The combinatorial theory of convex polytopes forms the basis of the combinatorial theory of triangulations. The most important theorem in combinatorics of polytopes is the upper bound theorem stating the maximal possible number of faces of polytopes with given number of vertices

[73]. This theorem on size was first proved using shelling [18], a total order for incremental construction of the boundary of a polytope.

Triangulations are similar to boundaries of polytopes in that they form simplicial complexes. However, theorems on (boundaries of) polytopes do not automatically generalize to theorems on triangulations, because triangulations might not be "convex" as polytopes. Indeed, the regular subclass of triangulations is the ones corresponding to (simplicial) polytopes and having convexity. When trying to generalize a theorem on polytopes to triangulations, it is important to distinguish what regularity means.

There have been several nice results on regular triangulations, but nonregular triangulations, the nonconvex ones, are still not understood. The third property we are interested in is the relation between *(non)regularity and view graph*.

One of the most important applications of polytope theory is linear programming, and the duality of linear programming is an important topic there. Our new method to understand regularity by view graph, uses linear programming duality to bridge the two.

Finally, we summarize our main results according to the three properties. Consult Chapters 2 to 5 for details.

- We analyze the following size or complexity:

  - the sizes of triangulations of specific polytopes (Theorem 2.2)

    * 3-polytopes as prisms, antiprisms

    * combinatorial d-cubes

  - the size gap between dissections and triangulations

    * the maximal side gap for 3-polytopes (Corollary 2.4)

    * the lower and upper bounds for the size of dissections of 3-polytopes (Proposition 2.7)

- As for regularity and view graph,

  - We study nonregular triangulations using view graphs:

    * A view graph describing in_front/behind relation viewed from a point is defined.

    * A triangulations having a contradicting cycle in a view graph view from some point becomes nonregular (Theorem 3.1).

    * However, there is an example showing the reverse implication fails (Examples 3.6).

- As for total orders for incremental construction,

  - We study unknown relations between total orders for incremental construction, shellability, extendable shellability and vertex decomposability.

    * We show examples showing differences of these classes, including minimal examples (Theorem 5.1, 5.2, Corollary 5.3).

    * We study relations among shellable but not extendably shellable examples, and showed properties of minimal such examples (Proposition 5.14).

* We propose an efficient algorithm for enumerating shellable 2-nonpseudomanifolds (Algorithm 5.20, Theorem 5.21).

– Incremental construciton orders for 2-spheres are also studied.

* Shellability is characterized (Theorem 4.2).

* Interesting sufficient condtions for geometric shellability are given (Theorem 4.4).

Chapter 2

Extremal properties for dissections of convex 3-polytopes

A dissection of a convex d-polytope is a partition of the polytope into d-simplices whose vertices are among the vertices of the polytope. Triangulations are dissections that have the additional property that the set of all its simplices forms a simplicial complex. The size of a dissection is the number of d-simplices it contains. This chapter compares triangulations of maximal size with dissections of maximal size. We also exhibit lower and upper bounds for the size of dissections of a 3-polytope and analyze extremal size triangulations for specific non-simplicial polytopes: prisms, antiprisms, Archimedean solids, and combinatorial d-cubes. (Joint work with Jesús A. De Loera and Francisco Santos [33])

2.1 Introduction

Let $\mathcal{A}$ be a point configuration in $\mathbb{R}^d$ with its convex hull conv($\mathcal{A}$) having dimension d. A set of d-simplices with vertices in $\mathcal{A}$ is a *dissection* of $\mathcal{A}$ if no pair of simplices has an interior point in common and their union equals conv($\mathcal{A}$). A dissection is a *triangulation* of $\mathcal{A}$ if in addition any pair of simplices intersects at a common face (possibly empty). The *size* of a dissection is the number of d-simplices it contains. We say that a dissection is *mismatching* when it is not a triangulation (i.e. it does not form a simplicial complex). In this chapter we study mismatching dissections of maximal possible size for a convex polytope and compare them with maximal triangulations. This investigation is related to the study of Hilbert bases and the hierarchy of covering properties for polyhedral cones which is relevant in Algebraic Geometry and Integer Programming (see [19] [41] [89]). Maximal dissections are relevant also in the enumeration of interior lattice points and its applications (see [4] [59] and references there).

It was first shown by Lagarias and Ziegler that dissections of maximal size turn out to be, in general, larger than maximal triangulations, but their example uses interior points [68]. Similar investigations were undertaken for mismatching minimal dissections and minimal triangulations of convex polytopes [5]. In this chapter we augment previous results by showing that it is possible to have *simultaneously*, in the same 3-polytope, that the size of a mismatching minimal (maximal) dissection is smaller (larger) than any minimal (maximal) triangulation. In addition, we show that the gap between the size of a mismatching maximal dissection and a maximal triangulation can grow linearly on the number of vertices and that this occurs already for a family of simplicial convex 3-polytopes. A natural question is how different are the upper and lower bounds for the size of mismatching dissections versus those bounds known for triangulations (see [84]). We prove lower and upper bounds on their size with respect to the number of vertices for dimension three and exhibit examples showing that our technique of proof fails already in dimension four. Here is the first summary of results:

Theorem 2.1.   *1. There exists an infinite family of convex simplicial 3-polytopes with increasing number of vertices whose mismatching maximal dissections are larger than their maximal triangulations. This gap is linear in the number of vertices (Corollary 2.4).*

   2. (a) There exists a lattice 3-polytope with 8 vertices containing no other lattice point other than its vertices whose maximal dissection is larger than its maximal triangulations.

   (b) There exists a 3-polytope with 8 vertices for which, simultaneously, its minimal dissection is smaller than minimal triangulations and maximal dissection is larger than maximal triangulations.

   (Proposition 2.5)

   3. If D is a mismatching dissection of a 3-polytope with n vertices, then the size of D is at least $n - 2$. In addition, the size of D is bounded above by $\binom{n-2}{2}$ (Proposition 2.7).

A consequence of our third point is that the result of [5], stating a linear gap between the size of minimal dissections and minimal triangulations, is best possible. The results are discussed in

Sections 2.2 and 2.3.

The last section presents a study of maximal and minimal triangulations for combinatorial d-cubes, three-dimensional prisms and anti-prisms, as well as other Archimedean polytopes. The following theorem and table summarize the main results:

Theorem 2.2.   *1. There is a constant $c > 1$ such that for every $d \geq 3$ the maximal triangulation among all possible combinatorial d-cubes has size at least $c^d d!$ (Proposition 2.10).*

   2. For a three-dimensional m-prism, in any of its possible coordinatizations, the size of a minimal triangulation is $2m - 5 + \lceil \frac{m}{2} \rceil$. For an m-antiprism, in any of its possible coordinatizations, the size of a minimal triangulation is $3m - 5$ (Proposition 2.12). The size of a maximal triangulation of an m-prism depends on the coordinatization, and in certain natural cases it is $(m^2 + m - 6)/2$ (Proposition 2.13).

   3. The following table specifies sizes of the minimal and maximal triangulations for some Platonic and Archimidean solids. These results were obtained via integer programming calculations using the approach described in [31]. All computations used the canonical symmetric coordinatizations for these polytopes [23]. The number of vertices is indicated in parenthesis (Remark 2.14):

P	$|T_{\min}(P)|$	$|T_{\max}(P)|$
Icosahedron (12)	15	20
Dodecahedron (20)	23	36
Cuboctahedron (12)	13	17
Icosidodecahedron (30)	45	?
Truncated Tetrahedron (12)	10	13
Truncated Octahedron (24)	27	?
Truncated Cube (24)	25	48
Small Rhombicuboctahedron (24)	35	?
Pentakis Dodecahedron (32)	54	?
Rhombododecahedron (14)	12	21

Table 2.1: Sizes of extremal triangulations of Platonic and Archimidean solids.

2.2   Maximal dissections of 3-polytopes

We introduce some important definitions and conventions: We denote by Q_m a convex m-gon with m an even positive integer. Let $v_1 v_2$ and $u_1 u_2$ be two edges parallel to Q_m, orthogonal to each other, on opposite sides of the plane containing Q_m, and such that the four segments $v_i u_j$ intersect the interior of Q_m. We suppose that $v_1 v_2$ and $u_1 u_2$ are not parallel to any diagonal or edge of Q_m. The convex hull P_m of these points has $m + 4$ vertices and it is a simplicial polytope. We will call north (respectively south) vertex of Q_m the one which maximizes (respectively minimizes) the scalar product with the vector $v_2 - v_1$. Similarly, we will call east (west) the vertex which maximizes (minimizes) the scalar product with $u_2 - u_1$. We denote these four vertices n, s, e and w, respectively. See Figure 2.1.
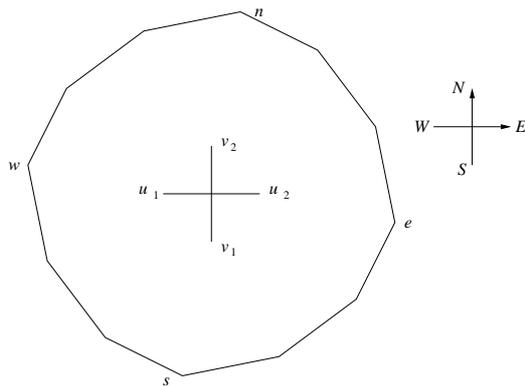
Figure 2.1: North, South, East, and West vertices.

We say that a directed path of edges inside Q_m is *monotone in the direction v_1v_2* (respectively u_1u_2) when the vertices of the path appear in the path following the same order given by the scalar product with $v_2 - v_1$ (respectively $u_2 - u_1$). An equivalent formulation is that any line orthogonal to v_1v_2 cuts the path in at most one point. We remark that by our choice of v_1v_2 and u_1u_2 all vertices of Q_m are ordered by the values of their scalar products with $v_2 - v_1$ and also with respect to $u_2 - u_1$. In the same way, a sequence of vertices of Q_m is *ordered in the direction* of v_1v_2 (respectively u_1u_2), if the order is the same as the one provided by using the values of the scalar products of the points with the vector $v_2 - v_1$ (respectively $u_2 - u_1$). Consider the two orderings induced by the directions of v_1v_2 and u_1u_2 on the set of vertices of Q_m. Let us call *horizontal* (respectively *vertical*) any edge joining two consecutive vertices in the direction of v_1v_2 (respectively of u_1u_2). As an example, if Q_m is regular then the vertical edges in Q_m form a zig-zag path as shown in Figure 2.2.
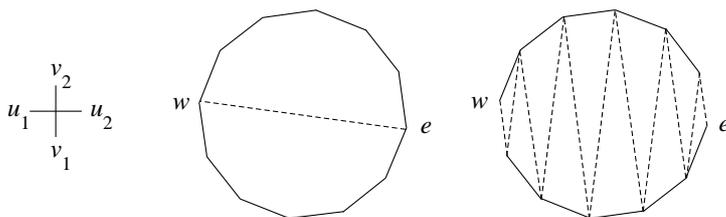
Figure 2.2: The minimal monotone path (middle) and the maximal monotone path made by the vertical edges (right) in the direction u_1u_2.

Our examples in this section will be based on the following observation and are inspired by a similar analysis of maximal dissections of dilated empty lattice tetrahedra in $\mathbb{R}^3$ by Lagarias and Ziegler [68]: Let R_m be the convex hull of the $m+2$ vertices consisting of the m-gon Q_m and v_1, v_2. R_m is exactly one half of the polytope P_m. Consider a triangulation T_0 of Q_m and a path Γ of edges of T_0 monotone with respect to the direction u_1u_2. Observe that Γ divides T_0 in two regions, which we will call the "north" and the "south". Then, the following three families of tetrahedra

form a triangulation T of R_m: the edges of Γ joined to the edge $v_1 v_2$; the southern triangles of T_0 joined to v_1; and the northern triangles of T_0 joined to v_2 (see Figure 2.3). Moreover, all the
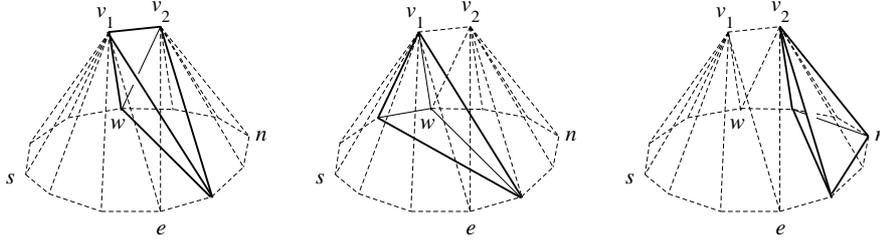
Figure 2.3: Three types of tetrahedra in R_m.

triangulations of R_m are obtained in this way: Any triangulation T of R_m induces a triangulation T_0 of Q_m. The link of $v_1 v_2$ in T is a monotone path of edges with respect to $u_1 u_2$ contained in T_0 and it divides T_0 in two regions, joined respectively to v_1 and v_2.

Using the Cayley trick, one can also think of the triangulations of R_m as the fine mixed subdivisions of the Minkowski sum $Q_m + v_1 v_2$ (see [54] and references within).

The size of a triangulation of R_m equals $m - 2 + |\Gamma|$, where $|\Gamma|$ is the number of edges in the path Γ. There is a unique minimal path in Q_m of length one (Figure 2.2, middle) and a unique maximal path of length $m - 1$ (Figure 2.2, right). Hence the minimal and maximal triangulations of R_m have, respectively, $m - 1$ and $2m - 3$ tetrahedra. The maximal triangulation is unique, but the minimal one is not: after choosing the diagonal in Γ the rest of the polygon Q_m can be triangulated in many ways. From the above discussion regarding R_m we see that we could independently triangulate each of the two halves of P_m with any number of tetrahedra from $m - 1$ to $2m - 3$. Hence, P_m has dissections of sizes going from $2m - 2$ to $4m - 6$. Among the triangulations of P_m, we will call *halving triangulations* those that triangulate the two halves of P_m. Equivalently, the halving triangulations are those which do not contain any of the four edges $v_i u_j$.

Proposition 2.3. *Let P_m be as described above, with Q_m being a regular m-gon. No triangulation of P_m has more than $\frac{7m}{2} + 1$ tetrahedra. On the other hand, there are mismatching dissections of P_m with $4m - 6$ tetrahedra.*

Proof. Let T be a triangulation of P_m. It is an easy application of Euler's formulas for the 3-ball and 2-sphere that the number of tetrahedra in a triangulation of any 3-ball without interior vertices equals the number of vertices plus interior edges minus three (such formula appears for instance in [39]). Hence our task is to prove that T has at most $\frac{5m}{2}$ interior edges. For this, we classify the interior edges according to how many vertices of Q_m they are incident to. There are only four edges not incident to any vertex of Q_m (the edges $v_i u_j$, $i, j \in \{1, 2\}$). Moreover, T contains at most $m - 3$ edges incident to two vertices of Q_m (i.e. diagonals of Q_m), since in any family of more than $m - 3$ such edges there are pairs which cross each other. Thus, it suffices to prove that T contains at most $\frac{3m}{2} - 1$ edges incident to just one vertex of Q_m, i.e. of the form $v_i p$ or $u_i p$ with $p \in Q_m$.

19

Let p be any vertex of Q_m. If p equals w or e then the edges pv_1 and pv_2 are both in the boundary of P_m; for any other p, exactly one of pv_1 and pv_2 is on the boundary and the other one is interior. Moreover, we claim that if pv_i is an interior edge in a triangulation T, then the triangle pv_1v_2 appears in T. This is so because there is a plane containing pv_i and having v_{3-i} as the unique vertex on one side. At the same time the link of pv_i is a cycle going around the edge. Hence, v_{3-i} must appear in the link of pv_i. It follows from the above claim that the number of interior edges of the form pv_i in T equals the number of vertices of Q_m other than w and e in the link of v_1v_2. In a similar way, the number of interior edges of the form pu_i in T equals the number of vertices of Q_m other than n and s in the link of u_1u_2. In other words, if we call $\Gamma_u = \mathrm{link}_T(v_1v_2) \cap Q_m$ and $\Gamma_v = \mathrm{link}_T(u_1u_2) \cap Q_m$ (the u, v in the index and of the vertices are reversed, because in this way Γ_u is monotone with respect to u_1u_2, and Γ_v with respect to v_1v_2), then the number of interior edges in T incident to exactly one vertex of Q_m equals $|\,\mathrm{vertices}(\Gamma_v)| + |\,\mathrm{vertices}(\Gamma_u)| - 4$. Our goal is to bound this number. As an example, Figure 2.4 shows the intersection of Q_m with a certain triangulation of P_m ($m = 12$). The link of v_1v_2 in this triangulation is the chain of vertices and edges $wabu_1nu_2ce$ (the star of v_1v_2 is marked in thick and grey in the figure). Γ_u consists of the chains wab and ce and the isolated vertex n. In turn, the link of u_1u_2 is the chain nv_1s and Γ_v consists of the isolated vertices n and s.
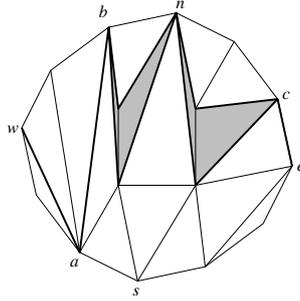
Figure 2.4: Illustration of the proof of Proposition 2.3.

Observe that Γ_v has at most three connected components, because it is obtained by removing from $\mathrm{link}_T(u_1u_2)$ (a path) the parts of it incident to v_1 and v_2, if any. Each component is monotone in the direction of v_1v_2 and the projections of any two components to a line parallel to v_1v_2 do not overlap. The sequence of vertices of Q_m ordered in the direction of v_1v_2, can have a pair of consecutive vertices contained in Γ_v only where there is a horizontal edge in Γ_v or in the at most two discontinuities of Γ_v.

We denote n_{hor} the number of horizontal edges in Γ_v and n'_{hor} this number plus the number of discontinuities in Γ_v (hence $n'_{hor} \leq n_{hor} + 2$). Every non-horizontal edge of Γ_v produces a jump of at least two in the v_1v_2-ordering of the vertices of P_m, hence we have

$$|\,\mathrm{vertices}(\Gamma_v)| - 1 - n'_{hor} \leq \frac{m - 1 - n'_{hor}}{2}.$$

Analogously, and with the obvious similar meaning for n_{vert} and n'_{vert},

20

$$| \operatorname{vertices}(\Gamma_u) | - 1 - n'_{vert} \leq \frac{m - 1 - n'_{vert}}{2}.$$

Since $\Gamma_u \cup \Gamma_v$ can be completed to a triangulation of Q_m, and exactly four non-interior edges of Q_m are horizontal or vertical, we have $n_{hor} + n_{vert} \leq (m - 3) + 4 = m + 1$, i.e. $n'_{hor} + n'_{vert} \leq m + 5$. Hence,

$$| \operatorname{vertices}(\Gamma_v) | + | \operatorname{vertices}(\Gamma_u) | \leq \left\lfloor \frac{2m + 2 + n'_{hor} + n'_{vert}}{2} \right\rfloor \leq \left\lfloor \frac{3m + 7}{2} \right\rfloor = \frac{3m}{2} + 3.$$

Thus, there are at most $\frac{3m}{2} - 1$ interior edges in T of the form pv_i or pu_i and at most $\frac{5m}{2}$ interior edges in total, as desired. □

Corollary 2.4. *The polytope P_m described above has the following properties:*

- *It is a simplicial 3-polytope with $m + 4$ vertices.*

- *Its maximal dissection has at least $4m - 6$ tetrahedra.*

- *Its maximal triangulation has at most $\frac{7m}{2} + 1$ tetrahedra.*

In particular, the gap between sizes of the maximal dissection and maximal triangulation is linear on the number of vertices.

Three remarks are in order: First, the size of the maximal triangulation for P_m may depend on the coordinates or, more specifically on which diagonals of Q_m intersect the tetrahedron $v_1 v_2 u_1 u_2$. Second, concerning the size of the minimal triangulation of P_m, we can easily describe a triangulation of P_m with only $m + 5$ tetrahedra: let the vertices n, s, e and w be as defined above (see Figure 2.1) and let us call northeast, northwest, southeast and southwest the edges in the arcs ne, nw, se and sw in the boundary of Q_m. Then, the triangulation consists of the five tetrahedra $v_1 v_2 u_1 u_2$, $v_1 v_2 u_1 w$, $v_1 v_2 u_2 e$, $v_1 u_1 u_2 s$ and $v_2 u_1 u_2 n$ (shown in the left part of Figure 2.5) together with the edges $v_2 u_2$, $v_2 u_1$, $v_1 u_2$ and $v_1 u_1$ joined, respectively, to the northeast, northwest, southeast and southwest edges of Q_m. The right part of Figure 2.5 shows the result of slicing through the triangulation by the plane containing the polygon Q_m.

Finally, although the corollary above states a difference between maximal dissections and maximal triangulations only for P_m with $m > 14$, experimentally we have observed there is a gap already for $m = 8$. Now we discuss two other interesting examples. The following proposition constitutes the proof of Theorem 2.1 (2).

Proposition 2.5. *1. Consider the following eight points in $\mathbb{R}^3$:*

- *The vertices $s = (0, 0, 0)$, $e = (1, 0, 0)$, $w = (0, 1, 0)$ and $n = (1, 1, 0)$ of a square in the plane $z = 0$.*

- *The vertices $v_1 = (-1, 0, 1)$ and $v_2 = (1, 1, 1)$ of a horizontal edge above the square, and*

- *The vertices $u_1 = (0, 1, -1)$ and $u_2 = (2, 0, -1)$ of a horizontal edge below the square.*
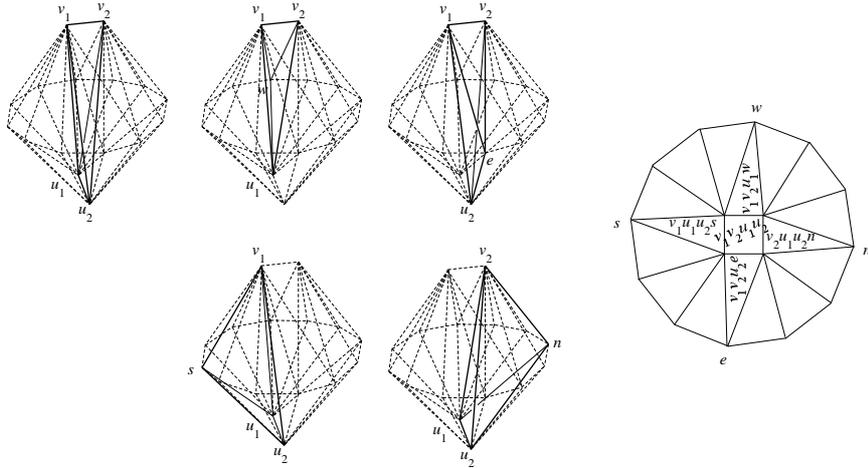
Figure 2.5: For the triangulation of P_m with $m + 5$ tetrahedra, its five central tetrahedra (left) and the intersection of the triangulation with the polygon Q_m (right) are shown. The four interior vertices are the intersection points of the edges $v_1 u_1$, $v_1 u_2$, $v_2 u_1$ and $v_2 u_2$ with the plane containing Q_m.

These eight points are the vertices of a polytope P whose only integer points are precisely its eight vertices and with the following properties:

(a) Its (unique) maximal dissection has 12 tetrahedra. All of them are unimodular, i.e. they have volume $1/6$.

(b) Its (several) maximal triangulations have 11 tetrahedra.

2. *For the 3-polytope with vertices $u_1 = (1, 0, 0)$, $w = (1, 0, 1)$, $v_1 = (-1, 0, 0)$, $s = (-1, 0, -1)$, $v_2 = (0, 1, 1)$, $n = (1, 1, 1)$, $u_2 = (0, 1, -1)$, $e = (-1, 1, -1)$, the sizes of its (unique) minimal dissection and (several) minimal triangulations are 6 and 7 respectively, and the sizes of its (several) maximal triangulations and (unique) maximal dissection are 9 and 10 respectively.*

Proof. The polytopes constructed are quite similar to P_4 constructed earlier except that Q_4 is non-regular (in part 2) and the segments $u_1 u_2$ and $v_1 v_2$ are longer and are not orthogonal, thus ending with different polytopes. The polytopes are shown in Figure 2.6. Figure 2.7 describes a maximal dissection of each of them, in five parallel slices. Observe that both polytopes have four vertices in the plane $y = 0$ and another four in the plane $y = 1$. Hence, the first and last slices in parts (a) and (b) of Figure 2.7 completely describe the polytope.

1. The vertices in the planes $y = 0$ and $y = 1$ form convex quadrangles whose only integer points are the four vertices. This proves that the eight points are in convex position and that the polytope P contains no integer point other than its vertices. Let us now prove the assertions on maximal dissections and triangulations of P:

(a) Consider the paths of length three $\Gamma_v = \{esnw\}$ and $\Gamma_u = \{sewn\}$, which are monotone respectively in the directions orthogonal to $v_1 v_2$ and $u_1 u_2$. Using them, we can construct two

22
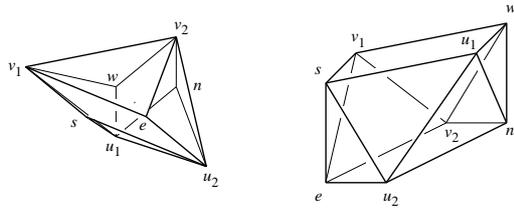
Figure 2.6: The two polytopes in Proposition 2.5.

$y = 0$ $y = .25$ $y = .5$ $y = .75$ $y = 1$

(a)

$y = 0$ $y = .25$ $y = .5$ $y = .75$ $y = 1$

(b)
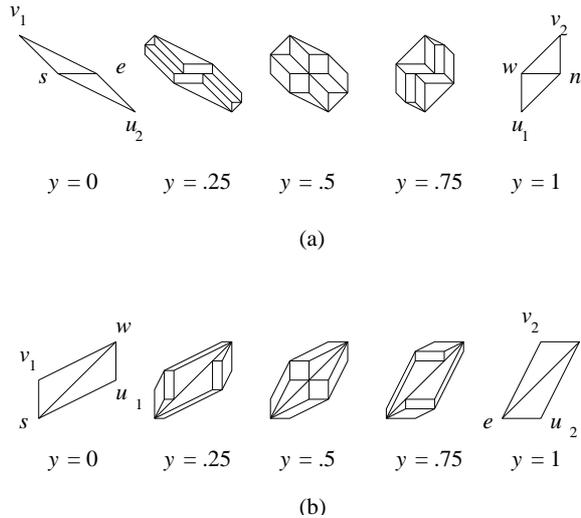
Figure 2.7: Five 2-dimensional slices of the maximal dissections of the polytopes in Proposition 2.5. The first and last slices are two facets of the polytopes containing all the vertices.

triangulations of size five of the polytopes $\mathrm{conv}(nsewv_1v_2)$ and $\mathrm{conv}(nsewu_1u_2)$, respectively. But they do not fill P completely. There is space left for the tetrahedra swv_1u_1 and env_2u_2. This gives a dissection of P with twelve tetrahedra. All the tetrahedra are unimodular, so no bigger dissection is possible.

(b) A triangulation of size 11 can be obtained using the same idea as above, but with paths Γ_v and Γ_u of lengths three and two respectively, which can be taken from the same triangulation of the square $nswe$.

To prove that no triangulation has bigger size, it suffices to show that P does not have any unimodular triangulation. Unimodularity means all tetrahedra have volume $1/6$. We start by recalling a well-known fact (see Corollary 4.5 in [90]). A lattice tetrahedron has volume $1/6$ if and only if each of its vertices v lies in a *consecutive* lattice plane parallel to the supporting plane of the opposite facet to v. Two parallel planes are said to be consecutive if their equations are $ax + by + cz = d$ and $ax + by + cz = d - 1$.

Suppose that T is a unimodular triangulation of P. We will first prove that the triangle u_1u_2e is in T. The triangular facet u_1u_2s of P, lying in the hyperplane $x + 2y + 2z = 0$, has to be joined to a vertex in the plane $x + 2y + 2z = 1$. The two possibilities are e and v_1. With the same argument,

if the tetrahedron $u_1u_2sv_1$ is in T, its facet $u_1u_2v_1$, which lies in the hyperplane $2x + 4y + 3z = 1$, will be joined to a vertex in $2x + 4y + 3z = 2$, and the only one is e. This finishes the proof that u_1u_2e is a triangle in T. Now, u_1u_2e is in the plane $x + 2y + z = 1$ and must be joined to a vertex in $x + 2y + z = 2$, i.e. to w. Hence u_1u_2ew is in T and, in particular, T uses the edge ew. P is symmetric under the rotation of order two on the axis $\{z = 0, x = \frac{1}{2}\}$. Applying this symmetry to the previous arguments we conclude that T uses the edge ns too. But this is impossible since the edges ns and ew cross each other.

2. This polytope almost fits the description of P_4, except for the fact that the edges v_1u_1, v_2u_2 intersect the boundary and not the interior of the planar quadrangle $nsew$. With the general techniques we have described, it is easy to construct halving dissections of this polytope with sizes from 6 to 10. Combinatorially, the polytope is a 4-antiprism. Hence, Proposition 2.12 shows that its minimal triangulation has 7 tetrahedra. The rest of the assertions in the statement were proved using the integer programming approach proposed in [31], which we describe in Remark 2.14. We have also verified them by enumerating all triangulations [82] [105]. It is interesting to observe that if we perturb the coordinates a little so that the planar quadrilateral $u_1v_1u_2e$ becomes a tetrahedron with the right orientation and without changing the face lattice of the polytope, then the following becomes a triangulation with ten tetrahedra: $\{u_1u_2se, u_1u_2ev_1, u_1u_2v_1w, u_1u_2wn, v_1v_2en, v_1v_2nw, u_1v_1se, v_1u_2ew, u_2wne, v_1wne\}$. $\qquad\square$

2.3 Bounds for the size of a dissection

Let D be a dissection of a d-polytope P. Say two $(d-1)$-simplices S_1 and S_2 of D *intersect improperly* in a $(d-1)$-hyperplane H if both lie in H, are not identical, and they intersect with non-empty relative interior. Consider the following auxiliary graph: take as nodes the $(d-1)$-simplices of a dissection, and say that two $(d-1)$-simplices are adjacent if they intersect improperly in certain hyperplane. A *mismatched region* is the subset of $\mathbb{R}^d$ that is the union of $(d-1)$-simplices over a connected component of size larger than one in such a graph. Later, in Proposition 2.9 we will show some of the complications that can occur in higher dimensions.

Define the *simplicial complex of a dissection* as all the simplices of the dissection together with their faces, where only faces that are identical (in $\mathbb{R}^d$) are identified. This construction corresponds intuitively to an *inflation* of the dissection where for each mismatched region we move the two groups of $(d-1)$-simplices slightly apart leaving the relative boundary of the mismatched region joined. Clearly, the simplicial complex of a dissection may be not homeomorphic to a ball.

The deformed d-simplices intersect properly, and the mismatched regions become holes. The numbers of vertices and d-simplices do not change.

Lemma 2.6. *All mismatched regions for a dissection of a convex 3-polytope P are convex polygons with all vertices among the vertices of P. Distinct mismatched regions have disjoint relative interiors.*

Proof. Let Q be a mismatched region and H the plane containing it. Since a mismatched region is a union of overlapping triangles, it is a polygon in H with a connected interior. If two triangles

forming the mismatched region have interior points in common, they should be facets of tetrahedra in different sides of H. Otherwise, the two tetrahedra would have interior points in common, contradicting the definition of dissection. Triangles which are facets of tetrahedra in one side of H cover Q. Triangles coming from the other side of H also cover Q.

Now, take triangles coming from one side. As mentioned above, they have no interior points in common. Their vertices are among the vertices of the tetrahedra in the dissection, thus among the vertices of the polytope P. Hence, the vertices of the triangles are in convex position, thus the triangles are forming a triangulation of a convex polygon in H whose vertices are among the vertices of P.

For the second claim, suppose there were distinct mismatched regions having an interior point in common. Then their intersection should be an interior segment for each. Let Q be one of the mismatched regions. It is triangulated in two different ways each coming from the tetrahedra in one side of the hyperplane. The triangles in either triangulation cannot intersect improperly with the interior segment. Thus the two triangulations of Q have an interior diagonal edge in common. This means the triangles in Q consists of more than one connected components of the auxiliary graph, contradicting the definition of mismatched region. □

Proposition 2.7. *1. The size of a mismatching dissection D of a convex 3-polytope with n vertices is at least $n - 2$.*

2. The size of a dissection of a 3-polytope with n vertices is bounded from above by $\binom{n-2}{2}$.

Proof. (1) Do an inflation of each mismatched region. This produces as many holes as mismatched regions, say m of them. Each hole is bounded by two triangulations of a polygon. This is guaranteed by the previous lemma. Denote by k_i the number of vertices of the polygon associated to the i-th mismatched region. In each of the holes introduce an auxiliary interior point. The point can be used to triangulate the interior of the holes by *filling in* the holes with the coning of the vertex with the triangles it sees. We now have a triangulated ball.

Denote by $|D|$ the size of the original dissection. The triangulated ball has then $|D| + \sum_{i=1}^{m} 2(k_i - 2)$ tetrahedra in total. The number of interior edges of this triangulation is the number of interior edges in the dissection, denoted by $e_i(D)$, plus the new additions, for each hole of length k_i we added k_i interior edges. In a triangulation T of a 3-ball with n boundary vertices and n' interior vertices, the number of tetrahedra $|T|$ is related to the number of interior edges e_i of T by the formula: $|T| = n + e_i - n' - 3$. The proof is a simple application of Euler's formula for triangulated 2-spheres and 3-balls and we omit the easy details.

Thus, we have the following equation:

$$|D| + \sum_{i=1}^{m} 2(k_i - 2) = n + e_i(D) + \sum_{i=1}^{m} k_i - m - 3.$$

This can be rewritten as $|D| = n + e_i(D) - \sum_{i=1}^{m} k_i + 3m - 3$. Taking into account that $e_i(D) \geq \sum_{i=1}^{m} 2(k_i - 3)$ (because diagonals in a polygon are interior edges of the dissection), we get an inequality

$$|D| \geq n + \sum_{i=1}^{m} k_i - 3m - 3.$$

Finally note that in a mismatching dissection we have $m \geq 1$ and $k_i \geq 4$. This gives the desired lower bound.

(2) Now we look at the proof of the upper bound on dissections. Given a 3-dissection, we add tetrahedra of volume zero to complete to a triangulation with flat simplices that has the same number of vertices. One can also think we are *filling in* the holes created by an inflation with (deformed) tetrahedra.

The lemma states that mismatched regions were of the shape of convex polygons. The 2-simplices forming a mismatched region were divided into two groups (those becoming apart by an inflation). The two groups formed different triangulations of a convex polygon, and they had no interior edges in common. In this situation, we can make a sequence of flips (see [70]) between the two triangulations with the property that any edge once disappeared does not appear again (see Figure 2.8). We add one abstract, volume zero tetrahedron for each flip, and obtain an abstract triangulation of a 3-ball.
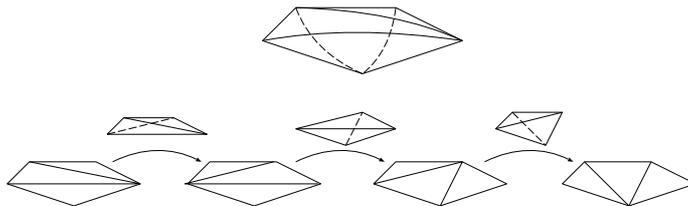
Figure 2.8: Filling in holes with tetrahedra according to flips.

The triangulation with flat simplices we created is a triangulated 3-ball with n vertices. By adding a new point in a fourth dimension, and coning from the boundary 2-simplices to the point, we obtain a triangulated 3-sphere containing the original 3-ball in its boundary. From the upper bound theorem for spheres (for an introduction to this topic see [106]) its size is bounded from above by the number of facets of a cyclic 4-polytope minus $2n - 4$, the number of 2-simplices in the boundary of D. The 4-dimensional cyclic polytope with $n + 1$ vertices is well-known to have $(n + 1)(n - 2)/2$ facets (see [49, page 63]), which completes the proof after a trivial algebraic calculation. □

Open problem 2.8. *What is the upper bound for sizes of dissections of d-dimensional polytopes with $d \geq 4$?*

In our proof of Proposition 2.7 we built a triangulated PL-ball from a three-dimensional dissection, using the flip connectivity of triangulations of a convex n-gon. Unfortunately the same cannot be applied in higher dimensions as the flip connectivity of triangulations of d-polytopes is known to be false for convex polytopes in general [86]. But even worse, the easy property we used from Lemma 2.6 that mismatched regions are convex polyhedra fails in dimension $d \geq 4$.

Proposition 2.9. *The mismatched regions of a dissection of a convex 4-polytope can be non-convex polyhedra.*

Proof. The key idea is as follows: suppose we have a 3-dimensional convex polytope P and two triangulations T_1 and T_2 of it with the following properties: removing from P the tetrahedra that T_1 and T_2 have in common, the rest is a non-convex polyhedron P' such that the triangulations T_1' and T_2' of it obtained from T_1 and T_2 do not have any interior 2-simplex in common (actually, something weaker would suffice: that their common interior triangles, if any, do not divide the interior of the polytope).

In these conditions, we can construct the dissection we want as a bipyramid over P, coning T_1 to one of the apices and T_2 to the other one. The bipyramid over the non-convex polyhedron P' will be a mismatched region of the dissection.

For a concrete example, start with Schönhardt's polyhedron whose vertices are labeled $1, 2, 3$ in the lower face and $4, 5, 6$ in the top face. This is a non-convex polyhedron made, for example, by twisting the three vertices on the top of a triangular prism. Add two antipodal points 7 and 8 close to the "top" triangular facets (those not breaking the quadrilaterals see Figure 2.9). For example, take as coordinates for the points $1 = (10, 0, 0)$, $2 = (-6, 8, 0)$, $3 = (-6, -8, 0)$, $4 = (10, -0.1, 10)$, $5 = (-6.1, 8, 10)$, $6 = (-5.9, -8.1, 10)$, $7 = (0, 0, 10.1)$, $8 = (0, 0, -0.1)$.
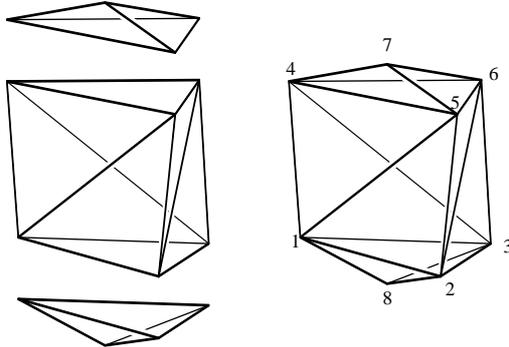
Figure 2.9: The mismatched region of a four-dimensional dissection.

Let P' be this non-convex polyhedron and let $T_1' = \{1278, 1378, 2378, 1247, 2457, 2357, 3567, 1367, 1467\}$ and $T_2' = \{4578, 4678, 5678, 1248, 2458, 2358, 3568, 1368, 1468\}$. T_1' cones vertex 7 to the rest of the boundary of P', and T_2' vertex 8. Any common interior triangle of T_1' and T_2' would use the edge 78. But the link of 78 in T_1' contains only the points 1, 2 and 3, and the link in T_2' contains only 4, 5 and 6.

Let P be the convex hull of the eight points, and let T_1 and T_2 be obtained from T_1' and T_2' by adding the three tetrahedra 1245, 2356 and 1346. $\qquad\square$

2.4 Optimal dissections for specific polytopes

The regular cube has been widely studied for its smallest dissections [52] [55]. This receives the name of *simplexity* of the cube. In contrast, because of the type of simplices inside a regular d-cube, a simple volume argument shows that the maximal size of a dissection is $d!$, the same as for triangulations. On the other hand, we know that the size of the maximal triangulation of a *combinatorial* cube can be larger than that: For example, the combinatorial 3-cube obtained as the prism over a trapezoid (vertices on a parabola for instance) has triangulations of size 7. Figure 2.10 shows a triangulation with 7 simplices for those coordinatizations where the edges AB and GH are not coplanar. The tetrahedron $ABGH$ splits the polytope into two non-convex parts, each of which can be triangulated with three simplices. To see this, suppose that our polytope is a very small perturbation of a regular 3-cube. In the regular cube, $ABGH$ becomes a diagonal plane which divides the cube into two triangular prisms $ABCDGH$ and $ABEFGH$. In the non-regular cube, the diagonals AH and BG, respectively, become non-convex. Any pair of triangulations of the two prisms, each using the corresponding diagonal, together with tetrahedron $ABGH$ give a triangulation of the perturbed cube with 7 tetrahedra. The boundary triangulation is shown in the flat diagram. It is worth noticing that for the regular cube the boundary triangulation we showed does not extend to a triangulation of the interior.
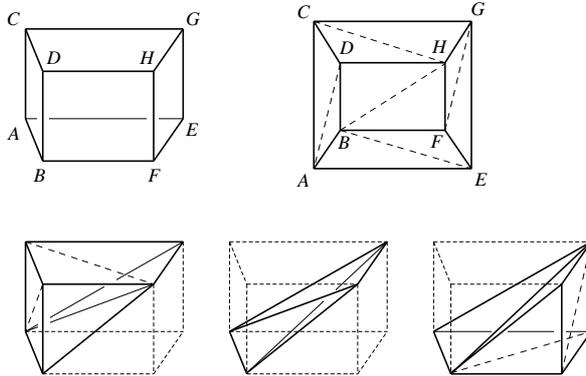
Figure 2.10: A triangulation of a combinatorial 3-cube into seven tetrahedra.

One can then ask, what is the general growth for the size of a maximal dissection of a combinatorial cube? To answer this question, at least partially, we use the above construction and we adapt an idea of M. Haiman, originally devised to produce small triangulations of regular cubes [52]. The idea is that from triangulations of a d_1-cube and a d_2-cube of sizes s_1 and s_2 respectively we can get triangulations of the $(d_1 + d_2)$-cube by first subdividing it into $s_1 \times s_2$ copies of the product of two simplices of dimensions d_1 and d_2 and then triangulating each such piece. We recall that any triangulation of the Cartesian product of a d_1-simplex and a d_2-simplex has $\binom{d_1+d_2}{d_1}$ maximal simplices. Hence, in total we have a triangulation of the $(d_1 + d_2)$-cube into $s_1 \times s_2 \times \binom{d_1+d_2}{d_1}$ maximal simplices. Recursively, if one starts with a triangulation of size s of the d-cube, one obtains triangulations for the rd-cube of size $(rd)!(\frac{s}{d!})^r$. In Haiman's context one wants s to be small, but

here we want it to be big.

More precisely, let us denote by $f(d)$ the function $\max_{C:\ d\text{-cube}}(\max_{T \text{ of } C} |T|)$ and call $g(d) = (f(d)/d!)^{1/d}$. Haiman's argument shows that if $f(d_1) \geq c_1{}^{d_1}d_1!$ and $f(d_2) \geq c_2{}^{d_2}d_2!$ for certain constants c_1 and c_2 then $f(d_1 + d_2) \geq c_1{}^{d_1}c_2{}^{d_2}(d_1 + d_2)!$. Put differently, that $g(d_1 + d_2) \geq (g(d_1)^{d_1}g(d_2)^{d_2})^{1/(d_1+d_2)}$. The value on the right hand side is the weighted geometric mean of $g(d_1)$ and $g(d_2)$. In particular, if both $g(d_1)$ and $g(d_2)$ are ≥ 1 and one of them is > 1 then $g(d_1 + d_2)$ is > 1 as well.

We have constructed above a triangulation of size 7 for the Klee-Minty 3-cube, which proves $g(3) \geq \sqrt[3]{7/6} = 1.053$. With Haiman's idea we can now construct "large" triangulations of certain 4-cubes and 5-cubes, which prove respectively that $g(4) \geq \sqrt[4]{7/6} = 1.039$ and $g(5) \geq \sqrt[5]{7/6} = 1.031$ (take $d_1 = 3$ and d_2 equal to one and two respectively). Finally, since any $d > 5$ can be expressed as a sum of 3's and 4's, we have $g(d) \geq \min\{g(3), g(4)\} \geq 1.039$ for any $d > 5$. Hence:

Proposition 2.10. *For the family of combinatorial d-cubes with $d > 2$ the function $f(d) = \max_{C:\ d\text{-cube}}(\max_{T \text{ of } C} |T|)$ admits the lower bound $f(d) \geq c^d d!$ where $c \geq 1.031$.*

Exactly as in Haiman's paper, the constant c can be improved (asymptotically) if one starts with larger triangulations for the smaller dimensional cubes. Using computer calculations (see Remark 2.14), we obtained a maximal triangulation for the Klee-Minty 4-cube with 38 maximal simplices, which shows that $g(d) \geq \sqrt[4]{38/24} = 1.122$ for every d divisible by 4 (see [2] for a complete study of this family of cubes). We omit listing the triangulation here but it is available from the author by request.

Open problem 2.11. *Is the sequence $g(d)$ bounded? In other words, is there an upper bound of type $c^d d!$ for the function $f(d)$? Remark that the same question for* minimal *triangulations of the regular d-cube (whether there is a lower bound of type $c^d d!$ for some $c > 0$) is open as well. See [94] for the best lower bound known.*

We continue our discussion with the study of optimal triangulations for three-dimensional prisms and antiprisms. We will call an *m-prism* any 3-polytope with the combinatorial type of the product of a convex m-gon with a line segment. An *m-antiprism* will be any 3-polytope whose faces are two convex m-gons and $2m$ triangles, each m-gon being adjacent to half of the triangles. Vertices of the two m-gons are connected with a band of alternately up and down pointing triangles.

Each such polyhedron has a regular coordinatization in which all the faces are regular polygons, and a realization space which is the set of all possible coordinatizations that yield the same combinatorial information [83]. Our first result is valid in the whole realization space.

Proposition 2.12. *For any three-dimensional m-prism, in any of its possible coordinatizations, the number of tetrahedra in a minimal triangulation is $2m - 5 + \lceil \frac{m}{2} \rceil$.*

For any three-dimensional m-antiprism, in any of its possible coordinatizations, the number of tetrahedra in a minimal triangulation is $3m - 5$.

Proof. In what follows we use the word *cap* to refer to the m-gon facets appearing in a prism or antiprism. We begin our discussion proving that any triangulation of the prism or antiprism has at least the size we state, and then we will construct triangulations with exactly that size.

We first prove that every triangulation of the m-prism requires at least $2m - 5 + \lceil \frac{m}{2} \rceil$ tetrahedra. We call a tetrahedron of the m-prism *mixed* if it has two vertices on the top cap and two vertices on the bottom cap of the prism, otherwise we say that the tetrahedron is *top-supported* when it has three vertices on the top (respectively *bottom-supported*). For example, Figure 2.11 shows a triangulation of the regular 12-prism, in three slices. Parts (a) and (c) represent, respectively, the bottom and top caps. Part (b) is the intersection of the prism with the parallel plane at equal distance to both caps. In this intermediate slice, bottom or top supported tetrahedra appear as triangles, while mixed tetrahedra appear as quadrilaterals.

<div align="center">(a)   (b)   (c)</div>
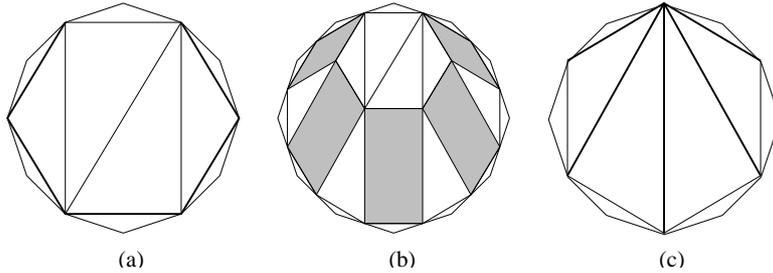
Figure 2.11: A minimal triangulation of the regular 12-prism.

Because all triangulations of an m-gon have $m - 2$ triangles there are always exactly $2m - 4$ tetrahedra that are bottom or top supported. In the rest, we show there are at least $\lceil \frac{m}{2} \rceil - 1$ mixed tetrahedra. Each mixed tetrahedra *marks* an edge of the top, namely the edge it uses from the top cap. Of course, several mixed tetrahedra could mark the same top edge. Group together top-supported tetrahedra that have the same bottom vertex. This grouping breaks the triangulated top m-gon into polygonal regions. Note that every edge between two of these regions must be marked. For example, in part (c) of Figure 2.11 the top cap is divided into 6 regions by 5 marked edges (the thick edges in the Figure). Let r equal the number of regions under the equivalence relation we set. There are $r - 1$ interior edges separating the r regions, and all of them are marked. Some boundary edges of the top cap may be marked too (none of them is marked in the example of Figure 2.11).

We can estimate the marked edges in another way: There are m edges on the boundary of the top, which appear partitioned among some of the regions (it could be the case some region does not contain any boundary edge of the m-gon). We claim that no more than *two* boundary edges per region will be unmarked (∗). This follows because a boundary edge is not marked only when the top supported tetrahedron that contains it has the point in the bottom cap that is directly under one of the vertices of the edge. In a region, at most two boundary edges can satisfy this. Hence we get at least $m - 2r$ marked edges on the boundary of the top and at least $(r - 1) + (m - 2r) = m - r - 1$ marked edges in total. Thus the number of mixed tetrahedra is at least the maximum of $r - 1$ and $m - r - 1$. In conclusion, we get that, indeed, the number of mixed tetrahedra is bounded below by $\lceil \frac{m}{2} \rceil - 1$. Note that we only use the combinatorics and convexity of the prism in our arguments. We will show that minimal triangulations achieve this lower bound, but then, observe that if m is even, in a minimal triangulation we must have $r = m/2$ and no boundary edge can be marked, as

<div align="center">30</div>

is the case in Figure 2.11. If m is odd, then we must have $r \in \{(m-1)/2, (m+1)/2\}$ and at most one boundary edge can be marked.

The proof that any triangulation of an m-antiprism includes at least $3m-5$ tetrahedra is similar. There are $2m-4$ top-supported and bottom-supported tetrahedra in any triangulation and there are $r-1$ marked edges between the regions in the top. The only difference is that, instead of claim (*), one has at most *one* unmarked boundary edge per region. Thus there are at least $m-r$ marked edges in the boundary of the top, and in total at least $(r-1)+(m-r) = m-1$ marked edges in the top. Hence there exist at least $(2m-4)+(m-1) = 3m-5$ tetrahedra in any triangulation.

For an m-antiprism we can easily create a triangulation of size $3m-5$ by choosing any triangulation of the bottom m-gon and then coning a chosen vertex v of the top m-gon to the $m-2$ triangles in that triangulation and to the $2m-3$ triangular facets of the m-antiprism which do not contain v. This construction is exhibited in Figure 2.12. Parts (a) and (c) show the bottom and top caps triangulated (each with its 5 marked edges) and part (b) an intermediate slice with the 5 mixed tetrahedra appearing as quadrilaterals.

(a)   (b)   (c)
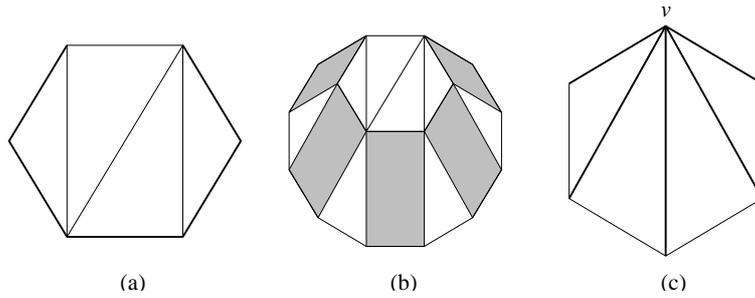
Figure 2.12: A minimal triangulation of the regular 6-antiprism.

For an m-prism, let u_i and v_i, $i = 1, \ldots, m$ denote the top and bottom vertices respectively, so that the vertices of each cap are labeled consecutively and $u_i v_i$ is always an edge of the prism.

If m is even we can chop off the vertices u_i for odd i and v_j for even j, so that the prism is decomposed into m tetrahedra and an $(\frac{m}{2})$-antiprism. The antiprism can be triangulated into $\frac{3m}{2} - 5$ tetrahedra, which gives a triangulation of the prism into $\frac{5m}{2} - 5$ tetrahedra, as desired. Actually, this is how the triangulation of Figure 2.11 can be obtained from that of Figure 2.12.

If m is odd we do the same, except that we chop off only the vertices $u_1, \ldots, u_{m-2}$ and $v_2, \ldots, v_{m-1}$ (no vertex is chopped in the edge $u_m v_m$). This produces $m-1$ tetrahedra and an $(\frac{m+1}{2})$-antiprism. We triangulate the antiprism into $\frac{3m+3}{2} - 5$ tetrahedra and this gives a triangulation of the m-prism into $\frac{5m+1}{2} - 5$ tetrahedra. $\qquad\square$

We have seen that the coordinates are not important when calculating minimal triangulations of the three-dimensional prisms and antiprisms. On the other hand, the difference in size of the maximal triangulation can be quite dramatic. Below we prove that in certain coordinatizations it is roughly $\frac{m^2}{2}$ and show experimental data indicating that for the regular prism it is close to $\frac{m^2}{4}$.

Proposition 2.13. *Let A_m be a prism of order m, with all its side edges parallel.*

31

1. *The size of a maximal triangulation of A_m is bounded as*

$$\left\lceil \frac{m^2 + 6m - 16}{4} \right\rceil \leq \max_{T \text{ of } A_m} |T| \leq \frac{m^2 + m - 6}{2}.$$

2. *The upper bound is achieved if the two caps (m-gon facets) are parallel and there is a direction in which the whole prism projects onto one of its side quadrangular facets. (For a concrete example, let one of the m-gon facets have vertices on a parabola and let A_m be the product of it with a segment).*

Proof. Let the vertices of the prism be labeled $u_1, \ldots, u_m$ and $v_1, \ldots, v_m$ so that the u_i's and the v_j's form the two caps, vertices in each cap are labeled consecutively and $u_i v_i$ is always a side edge.

For the upper bound in part (1), we have to prove that a triangulation of A_m has at most $\frac{m^2+m-6}{2} - 2m + 3 = \frac{m(m-3)}{2}$ interior diagonals. The possible diagonals are the edges $u_i v_j$ where $i - j$ is not in $\{-1, 0, 1\}$ modulo m. This gives exactly twice the number we want. But for any i and j the diagonals $u_i v_j$ and $u_j v_i$ intersect, so only one of them can appear in each triangulation.

We now prove that the upper bound is achieved if A_m is in the conditions of part (2). In fact, the condition on A_m that we will need is that for any $1 \leq i < j \leq k < l \leq m$, the point v_j sees the triangle $v_i u_k u_l$ from the same side as v_k and v_l (i.e. "from above" if we call top cap the one containing the v_i's). With this we can construct a triangulation with $\frac{m^2+m-6}{2} = \binom{m-1}{2} + 2m - 4$ tetrahedra, as follows:

First cone the vertex v_1 to any triangulation of the bottom cap (this gives $m - 2$ tetrahedra). The $m - 2$ upper boundary facets of this cone are visible from v_2, and we cone them to it (again $m - 2$ tetrahedra). The new $m - 2$ upper facets are visible from v_3 and we cone them to it ($m - 2$ tetrahedra more). Now, one of the upper facets of the triangulation is $v_1 v_2 v_3$, part of the upper cap, but the other $m - 3$ are visible from v_4, so we cone them and introduce $m - 4$ tetrahedra. Continuing the process, we will introduce $m - 4, m - 5, \ldots, 2, 1$ tetrahedra when coning the vertices $v_5, v_6, \ldots, v_{m-1}, v_m$, which gives a total of $\binom{m-1}{2} + 2m - 4$ tetrahedra, as desired.

The triangulation we have constructed is the *placing triangulation* [70] associated to any ordering of the vertices finishing with $v_1, \ldots, v_m$. A different description of the same triangulation is that it cones the bottom cap to v_1, the top cap to u_m, and its mixed tetrahedra are all the possible $v_i v_{i+1} u_j u_{j+1}$ for $1 \leq i < j \leq m - 1$. This gives $\binom{m-1}{2}$ mixed tetrahedra, and $\binom{m-1}{2} + 2m - 4$ tetrahedra in total.

We finally prove the lower bound stated in part (1). Without loss of generality, we can assume that our prism has its two caps parallel (if not, do a projective transformation keeping the side edges parallel). Then, A_m can be divided into two prisms in the conditions of part (2) of sizes k and l with $k + l = m + 2$: take any two side edges of A_m which posses parallel supporting planes and cut A_m along the plane containing both edges. By part (2), we can triangulate the two subprisms with $\binom{k+1}{2} - 3$ and $\binom{l+1}{2} - 3$ tetrahedra respectively, taking care that the two triangulations use the same diagonal in the dividing plane. This gives a triangulation of A_m with $\binom{k+1}{2} + \binom{l+1}{2} - 6 = \frac{k^2+l^2+m-10}{2}$ tetrahedra. This expression achieves its minimum when k and l are as similar as possible, i.e. $k = \lfloor \frac{m}{2} \rfloor + 1$ and $l = \lceil \frac{m}{2} \rceil + 1$. Plugging these values in the expression gives a triangulation of size $\left\lceil \frac{m^2+6m-16}{4} \right\rceil$. $\qquad \square$

Based on an integer programming approach we can compute maximal triangulations of specific polytopes (see remark at the end of this chapter). Our computations with regular prisms up to $m = 12$ show that the size of their maximal triangulations achieve the lower bound stated in part (1) of Proposition 2.13 (see Table 2.2). In other words, that the procedure of dividing them into two prisms of sizes $\lfloor \frac{m}{2} \rfloor + 1$ and $\lceil \frac{m}{2} \rceil + 1$ in the conditions of part (2) of Proposition 2.13 and triangulating the subprisms independently yields maximal triangulations.

We have also computed maximal sizes of triangulations for the regular m-antiprisms up to $m = 12$, which turn out to follow the formula $\left\lfloor \frac{m^2+8m-16}{4} \right\rfloor$. A construction of a triangulation of this size for every m can be made as follows: Let the vertices of the regular m-antiprism be labeled $u_1, \ldots, u_m$ and $v_1, \ldots, v_m$ so they are forming the vertices of the two caps consecutively in this order and $v_i u_i$ and $u_i v_{i+1}$ are side edges. We let $v_{m+1} = v_1$. The triangulation is made by placing the vertices in any ordering finishing with $v_1, v_2, v_m, v_3, v_{m-1}, \ldots, v_{\lceil \frac{m}{2} \rceil + 1}$. The tetrahedra used are the bottom-supported tetrahedra with apex v_1, top-supported tetrahedra with apex $u_{\lceil \frac{m}{2} \rceil}$ and the mixed tetrahedra $v_i v_{i+1} u_j u_{j+1}$ for $1 \le i \le j \le \lfloor \frac{m}{2} \rfloor$ and $u_i u_{i+1} v_j v_{j+1}$ for $\lfloor \frac{m}{2} \rfloor + 1 \le i < j \le m$.

We conjecture that these formulas for regular base prisms and antiprisms actually give the sizes of their maximal triangulations for every m, but we do not have a proof.

m	3	4	5	6	7	8	9	10	11	12
Prism (regular base)	3	6	10	14	19	24	30	36	43	50
Antiprism (regular base)	4	8	12	17	22	28	34	41	48	56

Table 2.2: Sizes of maximal triangulations of prisms and antiprisms.

Remark 2.14. How can one find minimal and maximal triangulations in specific instances? The approach we followed for computing Tables 2.1 and 2.2 and some of the results in Proposition 2.5 is the one proposed in [31], based on the solution of an integer programming problem. We think of the triangulations of a polytope as the vertices of the following high-dimensional polytope: Let A be a d-dimensional polytope with n vertices. Let N be the number of d-simplices in A. We define P_A as the convex hull in $\mathbb{R}^N$ of the set of incidence vectors of all triangulations of A. For a triangulation T the *incidence vector* v_T has coordinates $(v_T)_\sigma = 1$ if $\sigma \in T$ and $(v_T)_\sigma = 0$ if $\sigma \notin T$. The polytope P_A is the *universal polytope* defined in general by Billera, Filliman and Sturmfels [7] although it appeared in the case of polygons in [27]. In [31], it was shown that the vertices of P_A are precisely the integral points inside a polyhedron that has a simple description in terms of the oriented matroid of A (see [31] for information on oriented matroids). The concrete integer programming problems were solved using *C-plex Linear Solver*^{TM}. The program to generate the linear constraints is a small C++ program written by Jesús A. De Loera and Samuel Peterson. Source code, brief instructions, and data files are available via ftp at **http://www.math.ucdavis.edu/~deloera**. An alternative implementation by A. Tajima is also available [101] [102]. He used his program to corroborate some of these results.

It should be mentioned that a simple variation of the ideas in [31] provides enough equations for an integer program whose feasible vertices are precisely the 0/1-vectors of dissections. The

incidence vectors of dissections of $conv(A)$, for a point set A, are just the 0/1 solutions to the system of equations $\langle x, v_T \rangle = 1$, where v_T's are the incidence vectors for every regular triangulation T of the Gale transform A^* (regular triangulations in the Gale transform are the same as chambers in A). Generating all these equations is as hard as enumerating all the chambers of A. Nevertheless, it is enough to use those equations coming from placing triangulations (see [87, Section 3.2]), which gives a total of about n^{d+1} equations if A has n points and dimension d.

2.5   Conclusion

The difference between dissections and triangulations starts from dimension three, and we have solved the fundamental case of 3-polytopes. Now we know size differences in minimal and maximal sides, and bounds also on the size of dissections. The next case to consider is for 4-polytopes, though the situation can be quite messy.

We have also analyzed extremal size triangulations for specific non-simplicial 3-polytopes and combinatorial d-cubes. One of the related open problems important for triangulations of 3-polytopes is the following:

- What is the computational complexity of calculating the size of a maximal triangulation?

Chapter 3

Nonregular triangulations, view graphs of triangulations, and linear programming duality

For a triangulation and a point, we define a directed graph representing the order of the maximal dimensional simplices in the triangulation viewed from the point. We prove that triangulations having a cycle the reverse of which is not a cycle in this graph viewed from some point are forming a (proper) subclass of nonregular triangulations. We use linear programming duality to investigate further properties of nonregular triangulations in connection with this graph. (Preliminary versions appeared in [103] [104].)

3.1 Introduction

Let $\mathcal{A} = \{\boldsymbol{p}_1, \ldots, \boldsymbol{p}_n\} \subset \mathbb{R}^d$ be a point configuration with its convex hull conv($\mathcal{A}$) being a d-dimensional polytope. A *triangulation* Δ *of* $\mathcal{A}$ is a geometric simplicial complex with its vertices among $\mathcal{A}$ and the union of its faces equal to conv($\mathcal{A}$). A triangulation is *regular* (or *coherent*) if it can appear as the projection of the lower faces of the boundary complex of a $(d+1)$-dimensional polytope in $\mathbb{R}^{d+1}$. If not, the triangulation is *nonregular*. (See, for example, [69] [106].)

Starting from the study of generalized hypergeometric functions, Gel'fand, Kapranov & Zelevinskiĭ showed that regular triangulations of a point configuration are forming a polytopal structure described by the secondary polytope [44] [45]. In connection with Gröbner bases, Sturmfels showed that initial ideals for the affine toric ideal determined by a point configuration correspond to the regular triangulations of the point configuration [99] [100]. Regular triangulations are a generalization of the Delaunay triangulation well known in computational geometry, and have also been used extensively in this field [35].

Though nonregular triangulations are known to be behaving differently from regular triangulations, they are not well understood yet. Santos showed a nonregular triangulation with no flips indicating that a flip graph can be disconnected, which never happens when restricted to regular triangulations [86]. Ohsugi & Hibi showed the existence of a point configuration with no unimodular regular triangulations, but with a unimodular nonregular triangulation [77]. Also, de Loera, Hoşten, Santos & Sturmfels showed that cyclic polytopes can have exponential number of nonregular triangulations compared to polynomial number of regular ones [31]. The aim of this chapter is to put some insight into nonregular triangulations.

In the sequel, we fix a triangulation Δ. For the triangulation Δ and a point $\boldsymbol{v}$ in $\mathbb{R}^d$, we define the *graph* $G_{\boldsymbol{v}}$ *of* Δ *viewed from* $\boldsymbol{v}$ as the directed graph with its vertices corresponding to the d-simplices in Δ and a directed edge $\overrightarrow{\sigma\tau}$ existing when σ, τ are adjacent and $\boldsymbol{v}$ belongs to the closed halfspace having the affine hull aff($\sigma \cap \tau$) as its boundary and including σ. When $\boldsymbol{v} \in \text{aff}(\sigma \cap \tau)$, both edges $\overrightarrow{\sigma\tau}, \overrightarrow{\tau\sigma}$ appear in $G_{\boldsymbol{v}}$. The graph $G_{\boldsymbol{v}}$ is a directed graph whose underlying undirected graph is the adjacency graph of the d-simplices in Δ. Of course, $G_{\boldsymbol{v}}$ might differ for different choices of $\boldsymbol{v}$. Though there are infinitely many choices of viewpoints $\boldsymbol{v}$, there are only finitely many view graphs $G_{\boldsymbol{v}}$.

A sequence of vertices $\sigma_1, \sigma_2, \ldots, \sigma_i, \sigma_1$ in $G_{\boldsymbol{v}}$ forms a *cycle* when $\overrightarrow{\sigma_1\sigma_2}, \ldots, \overrightarrow{\sigma_{i-1}\sigma_i}, \overrightarrow{\sigma_i\sigma_1}$ are edges of $G_{\boldsymbol{v}}$ and $\sigma_i \neq \sigma_j$ for $i \neq j$. We define a cycle $\sigma_1, \sigma_2, \ldots, \sigma_i, \sigma_1$ to be *contradicting* when the reverse sequence $\sigma_1, \sigma_i, \ldots, \sigma_2, \sigma_1$ is not a cycle in $G_{\boldsymbol{v}}$. For vertices $\sigma_1, \ldots, \sigma_i$ in $G_{\boldsymbol{v}}$, the edges $\overrightarrow{\sigma_1\sigma_2}, \ldots, \overrightarrow{\sigma_{i-1}\sigma_i}, \overrightarrow{\sigma_2\sigma_1}, \ldots, \overrightarrow{\sigma_i\sigma_{i-1}}$ exist if and only if $\boldsymbol{v} \in \text{aff}(\sigma_1 \cap \cdots \cap \sigma_i)$.

The regularity of a triangulation can be stated as a linear programming problem, so regularity and linear programming obviously have a connection. An interesting point in our argument is that we use linear programming duality to analyze in further detail some properties of nonregular triangulations.

For any triangulation, the condition of regularity can be written as a linear programming problem as follows. Let the variable $\boldsymbol{w} = (w_1, \ldots, w_n)$ represent the $(d+1)$-coordinates of the lifting (or weight) of the vertices $\boldsymbol{p}_1, \ldots, \boldsymbol{p}_n$, such that the triangulation is lifted to a piecewise

linear function $f_{\boldsymbol{w}}$ from conv($\mathcal{A}$) to $\mathbb{R}$. For each $(d-1)$-simplex in Δ not in the boundary of the convex hull conv($\mathcal{A}$), the local convexity of $f_{\boldsymbol{w}}$ can be expressed by a linear inequality involving only the vertices of the two adjacent d-simplices in Δ (see Section 3.2.1). Gather the inequality constraints that correspond to each such interior $(d-1)$-simplex. Altogether, we get a system of inequalities $A\boldsymbol{w} > \boldsymbol{0}$ ($\boldsymbol{0}$ is the zero vector), and the triangulation is regular if and only if this has a solution. Easily, this is equivalent to $A\boldsymbol{w} \geq \boldsymbol{1}$ ($\boldsymbol{1}$ is the vector with all entries one) having a solution. Thus, by linear programming duality (or Farkas' lemma), the triangulation is nonregular if and only if the *dual problem* $\boldsymbol{u}A = \boldsymbol{0}$, $\boldsymbol{u} \geq \boldsymbol{0}$ has a nonzero solution.

Our main theorem constructs a nonzero solution of the dual problem combinatorially and explicitly from a contradicting cycle in a graph of the triangulation viewed from some point.

Theorem 3.1. *For a triangulation Δ, if a graph $G_{\boldsymbol{v}}$ viewed from some point $\boldsymbol{v}$ contains a contradicting cycle, in correspondence with this cycle, we can make a nonzero solution of the dual problem stated above. Thus, Δ is nonregular. The support set (i.e. collection of nonzero elements) of this solution becomes a subset of the edges forming the cycle. On the other hand, the reverse of this claim is not true. There exists a nonregular triangulation with none of its view graphs $G_{\boldsymbol{v}}$ containing a contradicting cycle. (See Example 3.6)*

The theorem says that triangulations containing a contradicting cycle in its graph $G_{\boldsymbol{v}}$ viewed from some point $\boldsymbol{v}$ are forming a (proper) subclass of nonregular triangulations. This subclass of triangulations On the other hand, regularity or nonregularity, defined by linear inequalities, is interesting in that their nonregularity are described more combinatorially using graphs. are of continuous nature. This is the first attempt to give a (combinatorial) subclass of nonregular triangulations. Even if we consider contradicting closed paths instead of contradicting cycles, allowing to pass the same vertex more than once, the class of the triangulations having such contradicting thing in its view graph does not change, because any contradicting closed path includes a contradicting cycle.

Checking that Example 3.6 is a counterexample for the reverse of the implication in the theorem (i.e. the view graph from any viewpoint does not contain a contradicting cycle), can be done by extensive enumeration of view graphs. However, by describing nonregularity as a linear programming problem, and using linear programming duality, we prove the counterexample in a more elegant way.

A similar but different directed graph of a triangulation viewed from a point has been studied by Edelsbrunner [36]. This was in the context of computer vision, and his graph represents the in_front/behind relation among simplices of any dimension, even not adjacent to each other. When our graph and the restriction of Edelsbrunner's graph to d-simplices are compared, neither includes the other in general. However, if we take the transitive closure of our graph, it includes his graph as a (possibly proper) subgraph. Our graph might be more appropriate in describing combinatorial structures of triangulations, because their underlying undirected graphs are the adjacency graphs of d-simplices. Edelsbrunner proves that if a triangulation is regular, his graph viewed from any point is "acyclic". The line shelling argument in a note there gives a proof for the contrapositive of our theorem, but without explicit construction of a solution of the dual problem.

We first prepare basic results, and then prove our main theorem (Section 3.2). Finally, we give illustrative examples and a counterexample for the reverse of the main theorem (Section 3.3).

3.2 Regularity, linear programming, and duality

3.2.1 Inequalities for regularity

A triangulation Δ of the point configuration $\boldsymbol{p}_1, \ldots, \boldsymbol{p}_n$ is regular if there exists a lifting (or weight) $w_1, \ldots, w_n \in \mathbb{R}$ such that the projection with respect to the x_{d+1} axis of the lower faces of the boundary complex of the $(d+1)$-dimensional polytope $\mathrm{conv}(\binom{\boldsymbol{p}_1}{w_1}, \ldots, \binom{\boldsymbol{p}_n}{w_n})$ becomes Δ. This condition on the lifting is equivalent to the condition that the function from $\mathrm{conv}(\mathcal{A})$ to $\mathbb{R}$ obtained by interpolating the lifting according to the triangulation in a piecewise linear fashion is convex. This implies (in fact, is equivalent to) the local convexity of this function in the neighborhood of every $(d-1)$-simplex in Δ which is not on the boundary of Δ. These conditions can be described by inequalities with $w_1, \ldots, w_n$ the variables.

A global criterion for convexity is therefore as follows:

- For each d-simplex $\mathrm{conv}(\boldsymbol{p}_{i_0}, \ldots, \boldsymbol{p}_{i_d})$ in Δ, and any point $\boldsymbol{p}_j \notin \{\boldsymbol{p}_{i_0}, \ldots, \boldsymbol{p}_{i_d}\}$, the lifted point $\binom{\boldsymbol{p}_j}{w_j}$ is above the hyperplane $\mathrm{aff}(\binom{\boldsymbol{p}_{i_0}}{w_{i_0}}, \ldots, \binom{\boldsymbol{p}_{i_d}}{w_{i_d}})$ in $\mathbb{R}^{d+1}$:

$$
\begin{vmatrix} 1 & \cdots & 1 \\ \boldsymbol{p}_{i_0} & \cdots & \boldsymbol{p}_{i_d} \end{vmatrix} \begin{vmatrix} 1 & \cdots & 1 & 1 \\ \boldsymbol{p}_{i_0} & \cdots & \boldsymbol{p}_{i_d} & \boldsymbol{p}_j \\ w_{i_0} & \cdots & w_{i_d} & w_j \end{vmatrix} > 0.
$$

A local criterion for convexity can be expressed with much fewer inequalities as follows:

- For each interior $(d-1)$-simplex $\mathrm{conv}(\boldsymbol{p}_{i_1}, \ldots, \boldsymbol{p}_{i_d})$ in Δ, where the two d-simplices $\mathrm{conv}(\boldsymbol{p}_{i_0}, \boldsymbol{p}_{i_1}, \ldots, \boldsymbol{p}_{i_d})$ and $\mathrm{conv}(\boldsymbol{p}_{i_1}, \ldots, \boldsymbol{p}_{i_d}, \boldsymbol{p}_{i_{d+1}})$ are intersecting, the lifted point $\binom{\boldsymbol{p}_{i_{d+1}}}{w_{i_{d+1}}}$ is above the hyperplane $\mathrm{aff}(\binom{\boldsymbol{p}_{i_0}}{w_{i_0}}, \ldots, \binom{\boldsymbol{p}_{i_d}}{w_{i_d}})$ in $\mathbb{R}^{d+1}$:

$$
\begin{vmatrix} 1 & \cdots & 1 \\ \boldsymbol{p}_{i_0} & \cdots & \boldsymbol{p}_{i_d} \end{vmatrix} \begin{vmatrix} 1 & \cdots & 1 & 1 \\ \boldsymbol{p}_{i_0} & \cdots & \boldsymbol{p}_{i_d} & \boldsymbol{p}_{i_{d+1}} \\ w_{i_0} & \cdots & w_{i_d} & w_{i_{d+1}} \end{vmatrix} > 0. \qquad (*)
$$

The equivalence of these two convexity conditions is proved easily by reducing to the one dimensional case.

The collection of inequalities $(*)$ for all interior $(d-1)$-simplices in Δ form a linear program which we denote by

$$
A\boldsymbol{w} > \boldsymbol{0}.
$$

We say the matrix A of this linear program *represents the regularity of* Δ. Note that this program has solutions if and only if the program $A\boldsymbol{w} \geq \boldsymbol{1}$ has solutions. Let m be the number of interior $(d-1)$-simplices in Δ. The matrix A is an $m \times n$ matrix.

Lemma 3.2. *For a triangulation Δ, and the matrix A representing its regularity, Δ is regular if and only if there exists $\boldsymbol{w} \in \mathbb{R}^n$ such that $A\boldsymbol{w} \geq \boldsymbol{1}$. By linear programming duality (or Farkas' lemma), Δ is nonregular if and only if there exists $\boldsymbol{u} \geq \boldsymbol{0}$, $\boldsymbol{u} \neq \boldsymbol{0}$ such that $\boldsymbol{u}A = \boldsymbol{0}$.*

Thus, the (non)regularity of Δ can be judged by the existence of a nonzero point in the polyhedron $\{\boldsymbol{u} \geq \boldsymbol{0} : \boldsymbol{u}A = \boldsymbol{0}\} \subset \mathbb{R}^m$ of the set of solutions of the dual problem.

3.2.2 A nonzero solution of the dual problem from a contradicting cycle

Here, we give an explicit construction of a nonzero solution of the dual problem $\boldsymbol{u}A = \boldsymbol{0}, \boldsymbol{u} \geq \boldsymbol{0}$, from a contradicting cycle in the graph $G_{\boldsymbol{v}}$ viewed from some point $\boldsymbol{v}$. For $\boldsymbol{v} \in \mathbb{R}^d$, a d-simplex σ in Δ, and $\boldsymbol{w} \in \mathbb{R}^n$, define $x_{d+1}(\boldsymbol{v}, \sigma, \boldsymbol{w})$ as follows: consider the projection along the $(d+1)$-coordinate of the point $\boldsymbol{v}$ to the affine hull of $f_{\boldsymbol{w}}(\sigma)$, the lifting of the d-simplex σ by $\boldsymbol{w}$, in $\mathbb{R}^{d+1}$, and let $x_{d+1}(\boldsymbol{v}, \sigma, \boldsymbol{w})$ be the x_{d+1} coordinate of this point.

Lemma 3.3. *Let Δ be a triangulation, A the matrix representing its regularity, and $\boldsymbol{v} \in \mathbb{R}^d$. For an edge $\overrightarrow{\sigma\tau}$ in the graph $G_{\boldsymbol{v}}$ viewed from $\boldsymbol{v}$, there exists a constant $\alpha_{\sigma\cap\tau} \geq 0$ such that*

$$x_{d+1}(\boldsymbol{v}, \sigma, \boldsymbol{w}) - x_{d+1}(\boldsymbol{v}, \tau, \boldsymbol{w}) = \alpha_{\sigma\cap\tau} A_{\sigma\cap\tau,*}\boldsymbol{w} \qquad (\text{for any } \boldsymbol{w} \in \mathbb{R}^n),$$

where $A_{\sigma\cap\tau,*}$ is the row of A corresponding to the interior $(d-1)$-simplex $\sigma\cap\tau$ in Δ. Furthermore, $\boldsymbol{v} \in \text{aff}(\sigma\cap\tau)$ if and only if $\alpha_{\sigma\cap\tau} = 0$.

Proof. Straightforward. □

We now construct a nonzero solution of the dual problem from a contradicting cycle. This will prove the forward implication in our main theorem.

Proof. **(Theorem 3.1)** Suppose we have a contradicting cycle $\sigma_1, \sigma_2, \ldots, \sigma_i, \sigma_1$ in $G_{\boldsymbol{v}}$. By Lemma 3.3, we can find $\alpha_{\sigma_1\cap\sigma_2}, \ldots, \alpha_{\sigma_i\cap\sigma_1} \geq 0$, or their collection as a vector $\boldsymbol{\alpha} \geq \boldsymbol{0}$, satisfying for any $\boldsymbol{w} \in \mathbb{R}^n$,

$$x_{d+1}(\boldsymbol{v}, \sigma_1, \boldsymbol{w}) - x_{d+1}(\boldsymbol{v}, \sigma_2, \boldsymbol{w})$$
$$\cdots$$
$$+ x_{d+1}(\boldsymbol{v}, \sigma_i, \boldsymbol{w}) - x_{d+1}(\boldsymbol{v}, \sigma_1, \boldsymbol{w})$$
$$= \alpha_{\sigma_1\cap\sigma_2} A_{\sigma_1\cap\sigma_2,*}\boldsymbol{w}$$
$$\cdots$$
$$+ \alpha_{\sigma_i\cap\sigma_1} A_{\sigma_i\cap\sigma_1,*}\boldsymbol{w}$$
$$= \boldsymbol{\alpha}A\boldsymbol{w}$$
$$= 0.$$

(The elements corresponding to the edges not in the cycle have 0 as their value in vector $\boldsymbol{\alpha}$.) Thus, $\boldsymbol{\alpha}A = \boldsymbol{0}$. Since we took a contradicting cycle, by Lemma 3.3, $\boldsymbol{\alpha} \neq \boldsymbol{0}$. Hence, we obtain a nonzero solution of the dual problem $\boldsymbol{u}A = \boldsymbol{0}, \boldsymbol{u} \geq \boldsymbol{0}$. This together with Lemma 3.2 proves the forward implication in the main theorem. □

3.2.3 Recognizing nonregularity or finding contradicting cycles

Judging whether the given triangulation Δ is (non)regular reduces to judging whether the system of inequalities $A\boldsymbol{w} \geq \boldsymbol{1}$ has a solution $\boldsymbol{w}$, where the matrix A represents the regularity of Δ in the sense described above. This is a linear programming problem, and can be computed in polynomial time for fixed dimension d, for example, using interior point method.

One way to judge if a triangulation Δ has a contradicting cycle in some view graph $G_{\boldsymbol{v}}$ is to enumerate all possible view graphs and enumerate the cycles there. The generation of view graphs can be done, for example, by generating all graphs viewed from the minimal cells in the hyperplane arrangement made by the affine hulls of the interior $(d-1)$-simplices in Δ.

3.3 Examples

Example 3.4 (A nonregular triangulation with 6 vertices). For the point configuration

$$\boldsymbol{p}_1 = (0\ 0), \qquad \boldsymbol{p}_2 = (4\ 0), \qquad \boldsymbol{p}_3 = (0\ 4),$$
$$\boldsymbol{p}_4 = (1\ 1), \qquad \boldsymbol{p}_5 = (2\ 1), \qquad \boldsymbol{p}_6 = (1\ 2),$$

we consider the triangulation Δ indicated in Figure 3.1(a) below. The graph $G_{\boldsymbol{v}}$ viewed from $\boldsymbol{v} = (\frac{4}{3}\ \frac{4}{3})$ is in Figure 3.1(b). It has one contradicting cycle $\boldsymbol{p}_1\boldsymbol{p}_4\boldsymbol{p}_5, \boldsymbol{p}_1\boldsymbol{p}_2\boldsymbol{p}_5, \boldsymbol{p}_2\boldsymbol{p}_5\boldsymbol{p}_6, \boldsymbol{p}_2\boldsymbol{p}_3\boldsymbol{p}_6, \boldsymbol{p}_3\boldsymbol{p}_4\boldsymbol{p}_6,$ $\boldsymbol{p}_1\boldsymbol{p}_3\boldsymbol{p}_4, \boldsymbol{p}_1\boldsymbol{p}_4\boldsymbol{p}_5$ denoted by bold edges. The matrix representing the regularity of Δ is

$$
A =
\begin{array}{c|cccccc}
 & w_1 & w_2 & w_3 & w_4 & w_5 & w_6 \\
\hline
\boldsymbol{p}_1\boldsymbol{p}_4 & 3 & & 1 & -8 & 4 & \\
\boldsymbol{p}_1\boldsymbol{p}_5 & -1 & 1 & & 4 & -4 & \\
\boldsymbol{p}_2\boldsymbol{p}_5 & 1 & 3 & & & -8 & 4 \\
\boldsymbol{p}_2\boldsymbol{p}_6 & & -1 & 1 & & 4 & -4 \\
\boldsymbol{p}_3\boldsymbol{p}_4 & 1 & & -1 & -4 & & 4 \\
\boldsymbol{p}_3\boldsymbol{p}_6 & & 1 & 3 & 4 & & -8 \\
\boldsymbol{p}_4\boldsymbol{p}_5 & 1 & & & -3 & 1 & 1 \\
\boldsymbol{p}_4\boldsymbol{p}_6 & & & 1 & 1 & 1 & -3 \\
\boldsymbol{p}_5\boldsymbol{p}_6 & & 1 & & 1 & -3 & 1 \\
\end{array}.
$$

(a) triangulation

(b) graph viewed from $\boldsymbol{v}$

(c) support of the dual solutions
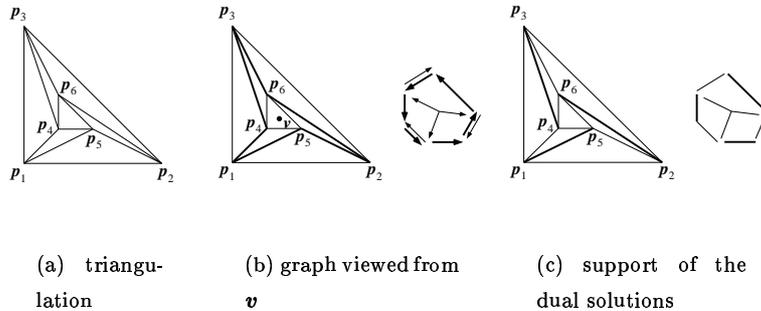
Figure 3.1: Example 3.4.

The polyhedron of the solutions of the dual problem is a single ray

$$\{\boldsymbol{u} \geq \boldsymbol{0} : A\boldsymbol{u} = \boldsymbol{0}\} = \mathbb{R}_{\geq 0}(0\,1\,0\,1\,1\,0\,0\,0\,0),$$

where interior 1-simplices are indexed lexicographically. The support of the nonzero solutions is denoted by bold edges in Figure 3.1(c). Remark that they are included in the (underlying undirected) edges of the contradicting cycle.

Example 3.5 (Another nonregular triangulation with 6 vertices). The vertex $\boldsymbol{p}_2$ in Example 3.4 is perturbed. The point configuration becomes

$$\boldsymbol{p}_1 = (0\,0), \qquad \boldsymbol{p}_2 = (\tfrac{7}{2}\,0), \qquad \boldsymbol{p}_3 = (0\,4),$$
$$\boldsymbol{p}_4 = (1\,1), \qquad \boldsymbol{p}_5 = (2\,1), \qquad \boldsymbol{p}_6 = (1\,2).$$

The triangulation Δ is indicated in Figure 3.2 below. Each of the graph viewed from $\boldsymbol{v}_1 = \left(\tfrac{5}{4}\,\tfrac{3}{2}\right)$, $\boldsymbol{v}_2 = \left(\tfrac{4}{3}\,\tfrac{4}{3}\right)$, or $\boldsymbol{v}_3 = \left(\tfrac{7}{5}\,\tfrac{7}{5}\right)$ has a unique contradicting cycle. The matrix representing the regularity of Δ is

$$A = \begin{array}{c|cccccc}
 & w_1 & w_2 & w_3 & w_4 & w_5 & w_6 \\
\hline
\boldsymbol{p}_1\boldsymbol{p}_4 & 3 & & 1 & -8 & 4 & \\
\boldsymbol{p}_1\boldsymbol{p}_5 & -1 & 1 & & \tfrac{7}{2} & -\tfrac{7}{2} & \\
\boldsymbol{p}_2\boldsymbol{p}_5 & \tfrac{1}{2} & 3 & & & -7 & \tfrac{7}{2} \\
\boldsymbol{p}_2\boldsymbol{p}_6 & & -1 & \tfrac{1}{2} & & 3 & -\tfrac{5}{2} \\
\boldsymbol{p}_3\boldsymbol{p}_4 & 1 & & -1 & -4 & & 4 \\
\boldsymbol{p}_3\boldsymbol{p}_6 & & 1 & \tfrac{5}{2} & 3 & & -\tfrac{13}{2} \\
\boldsymbol{p}_4\boldsymbol{p}_5 & 1 & & & -3 & 1 & 1 \\
\boldsymbol{p}_4\boldsymbol{p}_6 & & & 1 & 1 & 1 & -3 \\
\boldsymbol{p}_5\boldsymbol{p}_6 & & 1 & & \tfrac{1}{2} & -\tfrac{5}{2} & 1 \\
\end{array}.$$
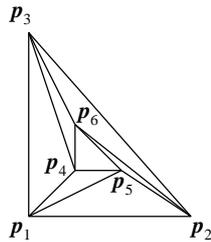
Figure 3.2: Triangulation of Example 3.5.

The polyhedron of the solutions of the dual problem is a cone

$$\{u \geq 0 : Au = 0\}$$

$$= \mathbb{R}_{\geq 0}(1\ 8\ 0\ 8\ 5\ 0\ 0\ 0\ 0)$$

$$+ \mathbb{R}_{\geq 0}(0\ 8\ 2\ 14\ 7\ 0\ 0\ 0\ 0)$$

$$+ \mathbb{R}_{\geq 0}(0\ 6\ 0\ 7\ 6\ 1\ 0\ 0\ 0)$$

$$+ \mathbb{R}_{\geq 0}(0\ 2\ 0\ 2\ 1\ 0\ 1\ 0\ 0)$$

$$+ \mathbb{R}_{\geq 0}(0\ 2\ 0\ 2\ 2\ 0\ 0\ 1\ 0)$$

$$+ \mathbb{R}_{\geq 0}(0\ 1\ 0\ 2\ 1\ 0\ 0\ 0\ 1),$$

where interior 1-simplices are indexed lexicographically. The first three rays correspond to the solutions made by the contradicting cycles in view graphs $G_{v_1}, G_{v_2}, G_{v_3}$, as in Subsection 3.2.2. The latter three rays have no such correspondence.

Example 3.6 (Counterexample for the reverse of the main theorem). With the point configuration

$$\boldsymbol{p}_1 = (0\ 0), \qquad \boldsymbol{p}_2 = (3\ 0), \qquad \boldsymbol{p}_3 = (3\ 4), \qquad \boldsymbol{p}_4 = (0\ 4),$$
$$\boldsymbol{p}_5 = (1\ 1), \qquad \boldsymbol{p}_6 = (2\ 1), \qquad \boldsymbol{p}_7 = (2\ 3), \qquad \boldsymbol{p}_8 = (1\ 3),$$

the triangulation Δ indicated in Figure 3.3(a) below is a nonregular triangulation with none of its view graphs $G_{\boldsymbol{v}}$ containing a contradicting cycle. The matrix representing the regularity of Δ is


(a) triangulation   (b) support of the dual solutions
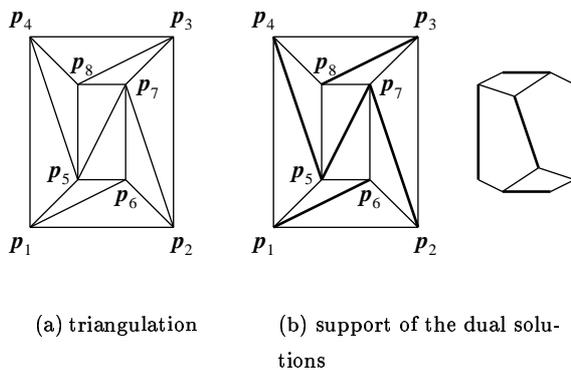
Figure 3.3: Example 3.6.

$$
A = \begin{array}{c|cccc|cccc}
 & w_1 & w_2 & w_3 & w_4 & w_5 & w_6 & w_7 & w_8 \\
\end{array}
$$

	w_1	w_2	w_3	w_4	w_5	w_6	w_7	w_8
p_1p_5	3			1	-8	4		
p_1p_6	-1	1			3	-3		
p_2p_6	2	4				-9	3	
p_2p_7		-2	2			4	-4	
p_3p_7		1	3				-8	4
p_3p_8			-1	1			3	-3
p_4p_8			2	4	3			-9
p_4p_5	2			-2	-4			4
p_5p_6	2				-4	1	1	
p_6p_7		2			2	-5	1	
p_7p_8			2		1		-4	1
p_5p_8				2	1		2	-5
p_5p_7					-2	2	-2	2

The polyhedron of the solutions of the dual problem is a single ray

$$\{ \boldsymbol{u} \geq \boldsymbol{0} : A\boldsymbol{u} = \boldsymbol{0} \} = \mathbb{R}_{\geq 0}(0\,2\,0\,1\,0\,2\,0\,1\,0\,0\,0\,0\,1),$$

where interior 1-simplices are indexed lexicographically. The support of the nonzero solutions is denoted by bold edges in Figure 3.3(b). If a contradicting cycle existed for some view graph G_v, this (directed) cycle should contain all of the bold edges (in its underlying undirected counterpart). However, there are no cycles containing all of these bold edges. Hence, there exists no view graph G_v containing a contradicting cycle for this example. (Remark: If we take the edge p_6p_8 instead of p_5p_7, this new flipped triangulation becomes regular.)

3.4 Conclusion

We defined a subclass of nonregular triangulations: triangulations having a contradicting cycle in a graph viewed from some point. This class is interesting in that their description is more combinatorial compared to regularity. This direction might lead to deeper understanding of nonregular triangulations. However, the work in this chapter is still premature. The ultimate goal is to give a combinatorial characterization of nonregularity. We first have to understand how much information the collection of all possible view graphs of a triangulation have. Important questions are as follows:

- Are there combinatorially isomorphic triangulations, one regular and one nonregular, having the same collection of view graphs?

- Can combinatorially isomorphic triangulations on point configurations with different oriented matroids have the same collection of view graphs?

Chapter 4

Geometric shellings of 3-polytopes

A total order of the facets of a polytope is a geometric shelling if there exists a combinatorially equivalent polytope in which the corresponding order of facets becomes a line shelling. The subject of this chapter is (geometric) shellings of 3-polytopes. Recently, a graph theoretical characterization of geometric shellings of 3-polytopes was given by Holt & Klee and Mihalisin & Klee.

- We first give a graph theoretical characterization of shellings of 3-polytopes.

Then we show interesting sufficient conditions for a shelling of a 3-polytope to be geometric:

- the first and the last facet being adjacent,

- any facet (except the first two) being adjacent to no less than two previous facets or

- the polytope being simple and only having triangular or quadrilateral facets.

A nongeometric shelling of a (simplicial) 3-polytope was first shown by Smilansky. Simple 3-polytopes allow perturbations of facets, thus might have more chance a shelling is geometric. However,

- we show an example of a simple 3-polytope having a nongeometric shelling. The number of facets of this example is minimal and smaller compared to those previously known.

The discussions proceed in the polar setting: as total orders of vertices of the polar polytope. The connection between our results on 3-polytopes and their proofs using graph theory is of interest. (Joint work with Takayuki Ishizeki [57])

4.1 Introduction

A total order of the facets of a polytope is a *shelling* if it satisfies some topological condition (defined below at (∗)). Shellings have many applications both in combinatorial and computational geometry: for example, they are crucial for the upper bound theorem [18] [73], and are used in convex hull construction [91]. A total order of the facets of a polytope corresponds to a total order of the vertices of the polar polytope. Such order of vertices is a *polar shelling*. A *line shelling* is some special shelling, and its polar becomes an ordering of the vertices of the polar polytope by a sweep of parallel hyperplanes, which we call a *polar line shelling* (see [40] [93] [106]). Polar line shellings are relevant to simplex methods in linear programming [88].

A total order of the facets of a polytope is a *geometric shelling* if in some combinatorially equivalent polytope the corresponding order becomes a line shelling. We call the total order of the vertices of the polar a *polar geometric shelling*. If a (polar) shelling is not a (polar) geometric shelling, it is called a *(polar) nongeometric shelling*.

In this chapter, we discuss combinatorial properties of shellings of 3-polytopes. In the beginning of this chapter, we listed our results in terms of shellings, or total order of facets. In the remaining main part, most of our discussions proceed in the polar setting: as total orders of the vertices of (a graph of) a 3-polytope. The face lattice of a 3-polytope is completely determined by its graph. The main results of this chapter can be described in purely graph theoretical terms. Holt & Klee [53] and Mihalisin & Klee [74] recently gave a characterization of polar geometric shellings of 3-polytopes in terms of directed graphs. Their results are used in some of our proofs.

Special cases of our interests are shellings of simple 3-polytopes (polar shellings of simplicial 3-polytopes). Such polytopes do not change their combinatorial properties under perturbation of facets (vertices). So, there might be more chance shellings (polar shellings) of such polytopes become geometric shellings (polar geometric shellings).

All graphs considered are simple (i.e. no loops or multiple edges). Connectivity means vertex connectivity.

The following is basic for graphs of 3-polytopes.

Lemma 4.1.   • (*Steinitz' theorem*) *A graph is a graph of a 3-polytope if and only if it is planar and 3-connected.*

• *A graph is a graph of a simplicial 3-polytope if and only if it is maximal planar and has no less than four vertices.*

Now, to directed graphs. A total order $<$ of the vertices of a graph induces a directed graph by directing $\overrightarrow{st}$ for an edge $\{s, t\}$ with $s < t$. Directed graphs by such directing are acyclic. The symbol k will be used for the cardinality of the vertices, and the vertices will be labeled $1 < \cdots < k$ according to the total order.

We define a total order $F_1, \ldots, F_k$ of the facets of a 3-polytope to be a *shelling* if

$$\bigcup_{j=1}^{i} F_j \cong B^2 \quad (1 \le i < k), \tag{∗}$$

where $\cong B^2$ means homeomorphic to a standard 2-dimensional ball. (This definition is compatible with the one in Section 5.2.) A total order of the vertices of a 3-polytope is a *polar shelling* if the corresponding order of the facets of the polar polytope is a shelling. The face lattice of a 3-polytope is determined by its graph. The graph of the polar of a 3-polytope is the dual of the graph of the original polytope. Since shellings and polar shellings are well-defined for the face lattice, (polar) shellings can be defined for graphs of 3-polytopes. We give a simple characterization for polar shellings:

Theorem 4.2. *A total order of the vertices of a graph of a 3-polytope is a polar shelling if and only if the induced directed graph has a unique source and a unique sink. (The source vertex 1, the sink vertex k.)*

Proof. Section 4.2. □

Since (polar) geometric shellings of 3-polytopes are also combinatorial properties depending only on the face lattice and the total order of the facets (or vertices), we can define them for graphs of 3-polytopes. A necessary and sufficient condition for a total order of the vertices of a graph of a 3-polytope to become a polar geometric shelling was given recently by Holt & Klee [53] and Mihalisin & Klee [74]:

Theorem 4.3 ([53] [74]). *A total order of the vertices of a graph of a 3-polytope is a polar geometric shelling if and only if the induced directed graph has a unique source, a unique sink (the source vertex 1 and the sink vertex k) and three independent paths from 1 to k.*

The paths in a directed graph should be monotone. Theorem 4.2 together with this theorem clarifies that the "geometric" part is corresponding to the existence of the three independent paths.

We define a total order $F_1, \ldots, F_k$ of the facets of a 3-polytope to be a *strong shelling* if it is a shelling and

$$F_i \cap \left(\bigcup_{j=1}^{i-1} F_j \right) \text{ is the union of no less than two edges} \quad (3 \leq i \leq k).$$

The corresponding order of the vertices of the polar is a *polar strong shelling*.

The following observations are of interest in context of 3-polytopes, though their proofs are direct after Theorem 4.3:

Theorem 4.4. *Each of the following conditions is sufficient for a polar shelling total order of the vertices of a graph G of a 3-polytope to be a polar geometric shelling.*

(i) *Vertices 1 and k are adjacent.*

(ii) *The total order is a polar strong shelling.*

(iii) *G is a graph of a simplicial 3-polytope with its degree at most 4.*

A nongeometric shelling of a 4-polytope was known and one of a 3-polytope was given by Smilansky [50] [93]. Both examples are for simplicial polytopes. In the polar setting, they become

polar nongeometric shellings of simple polytopes. Simplicial 3-polytopes allow perturbations of vertices, thus might have more chance a polar shelling is polar geometric. However, we give a polar nongeometric shelling of a simplicial 3-polytope with 6 vertices and 8 facets. The number of vertices of this example is minimal and smaller compared to those previously known (Example 4.7).

The remaining details are given in Section 4.2.

4.2 Proofs, examples and remarks

Proof. **(Theorem 4.2)**

only if: Suppose the total order was a polar shelling. By definition $(*)$ of shelling, any vertex $i > 1$ is adjacent to a smaller vertex. Thus the only source is 1. The reverse order of a shelling is also a shelling, because the boundary of a 3-polytope is homeomorphic to a 2-sphere, and removing a 2-ball from a 2-sphere results in a 2-ball. So, similarly, the only sink is k.

if: Suppose the induced directed graph had a unique source and a unique sink. Suppose the condition $(*)$ for shelling was satisfied for $i = 1, \ldots, r-1$, but violated for r (> 1). If $A = F_r \cap (\bigcup_{j=1}^{r-1} F_j)$ is empty or a vertex, r is also a source, contradicting the assumption. Thus, A should consist of no less than two connected components. Take a polytope with facets $F_1, \ldots, F_k$ realizing the situation. There exists a Jordan arc in $\bigcup_{j=1}^{r} F_j$ having in each side (interior points of) some facet F_j $(j > r)$. Hence, there should be at least one sink in each side, contradicting the assumption.

$\square$

The "if" proof is not valid for dimension larger than 3. Indeed, we have a counterexample in dimension 4. For this case, replace $\cong B^2$ in the definition $(*)$ of shelling by $\cong B^3$, homeomorphic to a 3-ball.

Example 4.5. *The 4-polytope with vertices*

$$p_1 = (0\ 0\ 0\ 0), \qquad p_2 = (2\ 0\ 0\ 0), \qquad p_3 = (0\ 6\ 0\ 0),$$
$$p_4 = (1\ 1\ 2\ 0), \qquad p_5 = (1\ 2\ 3\ 0), \qquad p_6 = (0\ 0\ 0\ 1)$$

is made by coning p_6 to the 3-polytope with vertices $p_1, \ldots, p_5$. The total order of the facets $\langle p_1p_2p_4p_6\rangle, \langle p_1p_4p_5p_6\rangle, \langle p_1p_3p_5p_6\rangle, \langle p_2p_3p_5p_6\rangle, \langle p_2p_4p_5p_6\rangle, \langle p_1p_2p_3p_4p_5\rangle, \langle p_1p_2p_3p_6\rangle$ forms a Hamiltonian path (indeed, a Hamiltonian cycle), thus the induced directed graph has a unique source and a unique sink. However, the union of the first four facets is not homeomorphic to B^3.

Remark 4.6. (i) *Theorem 4.4(i) is not true in dimension 4. Smilansky's treatment [93] of a polytope in Grünbaum & Sreedharan's list [50] shows a nongeometric shelling of a simplicial 4-polytope with the first and the last facet adjacent.*

(ii) *A strong shelling of a simplicial 3-polytope with the first and last vertex adjacent is equivalent to "a shelling order of vertices" in [28] [29].*

(iii) *The only graph of a simple 3-polytope (i.e. planar, 3-connected and degree 3) which has a polar strong shelling is K_4.*

(iv) *By Euler's formula, graphs of simplicial 3-polytopes satisfying the condition in Theorem 4.4(iii) have 6 vertices at most. The unique (combinatorial types of) graphs of simplicial 3-polytopes with 4 or 5 vertices have degree at most 4. One type of the graphs of simplicial 3-polytopes with 6 vertices has degree at most 4. It can also be checked directly that every polar shelling of the vertices of these three types of graphs satisfying the condition in Theorem 4.4(iii) is a polar geometric shelling.*

Example 4.7. *The figure shows an example of a polar nongeometric shelling of a simplicial 3-polytope. Since the total order is defining a Hamiltonian path, it is a shelling. This example has 6 vertices and 8 facets.*

This example is minimal with respect to the number of vertices, because no 3-polytope with less than 6 vertices has a polar nongeometric shelling: The graph of a 3-polytope with 4 vertices is K_4, thus of a simplicial 3-polytope. Any total order of its vertices is a polar geometric shelling. There are two combinatorial types of graphs of 3-polytopes with 5 vertices, one of a simplicial 3-polytope and the other not. Any polar shelling of the vertices of these graphs is a polar geometric shelling. (There also exist other 3-polytopes with 6 vertices having polar nongeometric shellings. Though not simplicial, the smallest number 5 of facets among them is attained by a triangular prism.)
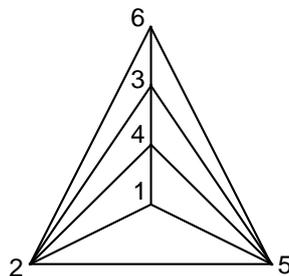
Example 4.8. *In the polar setting, Smilansky's example [93] is a polar nongeometric shelling of a simple 3-polytope. It has 8 vertices and 6 facets.*
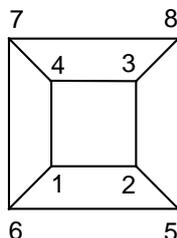
4.3 Conclusion

We gave a characterization of polar shellings of 3-polytopes. The characterization of polar geometric shellings of 3-polytopes was already settled by [53] [74]. We supplemented their results with a few sufficient conditions of interest in polytope theory. Asking these questions for 4-polytopes is a possible but probably difficult generalization [106]. Direct generalizations do not work (Remark

4.6(i)). One might need to look first for a proper question to ask. Among polytopes with a polar shelling which is not a polar geometric shelling, the one having minimal number of vertices was also given.

Chapter 5

Incremental construction properties in dimension two—shellability, extendable shellability and vertex decomposability

We give new examples of shellable but not extendably shellable two dimensional simplicial complexes. They include minimal examples, which are smaller than those previously known. We also give new examples of shellable but not vertex decomposable two dimensional simplicial complexes. Among them are extendably shellable ones. This shows that neither extendable shellability nor vertex decomposability implies the other. We found these examples by enumerating shellable two dimensional simplicial complexes which are not pseudomanifolds. A rather efficient algorithm for this enumeration is also given. (Joint work with Sonoko Moriyama [76])

5.1 Introduction

A pure simplicial complex is *shellable* if there is a total order of facets according to which the facets can be pasted incrementally in a nice way (see Section 5.2 for definitions). The shellability of the boundary complexes of polytopes was shown by Bruggesser & Mani [18]. Shellability is important both in combinatorial and computational geometry, for example, it was essential for the proof of the upper bound of the number of faces of polytopes [73], or has been used for efficient convex hull construction of polytopes [91]. Shellability has also been studied from algebra through the Stanley-Reisner ring of simplicial complexes [34] [92].

A pure simplicial complex is *extendably shellable* if any sequence of a subset of facets satisfying the condition of being pasted nicely can be continued to a shelling. This means we can make a shelling by pasting facets one by one in a greedy manner. Extendable shellability was defined by Danaraj & Klee [25], who showed that for a 2-pseudomanifold, shellability, extendable shellability, and being a 2-ball or a 2-sphere are equivalent [26]. It is also known that rank 3 (i.e. geometrically, 2-dimensional) matroids are extendably shellable [14]. However, a 3-pseudomanifold, or even the boundary complex of a 4-polytope can be shellable but not extendably shellable [107]. Even in dimension two, if we consider simplicial complexes other than pseudomanifolds, shellable but not extendably shellable examples exist [12, Exercise 7.37] [51, Section 5.3] [92]. Since, for a 1-simplicial complex, or a graph, shellability, extendable shellability and connectivity are equivalent, dimension two is the smallest interesting case to consider. (For more information on shellability, extendable shellability and other combinatorial topological properties, see [13] [25] [97] [106] [107]).

The first topic of this chapter is shellable but not extendably shellable 2-simplicial complexes (Section 5.3). First, we give new examples of such kind. Among them are examples smaller than those in the literature, and we have checked their minimality by enumeration:

Theorem 5.1. *The two 2-simplicial complexes V6F9-1, 2 with 6 vertices and 9 facets are shellable but not extendably shellable (Example 5.5). There is no 2-simplicial complex with less than 6 vertices or less than 9 facets having this property.*

Next, we show operations to make larger shellable but not extendably shellable 2-simplicial complexes from smaller ones, and show the relation among the examples with respect to these operations or set inclusion (Propositions 5.10, 5.14, Remark 5.11).

A pure simplicial complex is *vertex decomposable* if there is a total order of vertices according to which the facets including the vertex can be nicely removed. This is another operation for breaking (or constructing) simplicial complexes inductively. Vertex decomposability was first introduced by Billera & Provan [11] [81] in connection with the Hirsch conjecture (see also [13]). Vertex decomposability implies shellability. If all boundary complexes of polytopes were vertex decomposable, then this implied the Hirsch conjecture. However, polyhedra whose boundary complexes are not vertex decomposable (but shellable) have been found [66] [81]. Shellable but not vertex decomposable simplicial complexes begin to exist from 2-simplicial complexes which are not pseudomanifolds [51, Section 5.3] [92].

The second topic of this chapter is shellable but not vertex decomposable 2-simplicial complexes

(Section 5.4). First, we give new examples of such kind. They have the same size as the smallest example in the literature, and we have checked their minimality by enumeration:

Theorem 5.2. *The three 2-simplicial complexes* `V6F10-1, 6, 7` *with* 6 *vertices and* 10 *facets are shellable but not vertex decomposable (Example 5.15). There is no 2-simplicial complex with less than* 6 *vertices or with* 6 *vertices and less than* 10 *facets having this property. Furthermore,* `V6F10-1` *is not extendably shellable, but* `V6F10-6, 7` *are extendably shellable.*

Vertex decomposable but not extendably shellable simplicial complexes have been known (`V6F11-3` [12, Exercise 7.37], for example). On the other hand, our extendably shellable but not vertex decomposable examples are new. From these examples, we know that these two properties stronger than shellability do not have logical implications each other:

Corollary 5.3. *Neither extendable shellability nor vertex decomposability implies the other (Corollary 5.16).*

The examples in this chapter were generated using a computer. In the final part (Section 5.5), we propose a rather efficient algorithm to enumerate shellable 2-simplicial complexes which are not pseudomanifolds (Algorithm 5.20, Theorem 5.21). It generates one example per each class consisting of those identical with respect to the relabeling of vertices.

The study in this chapter is an expansion of [75].

5.2 Definitions and basic properties

Let $V = \{1, \ldots, n\}$ be a finite set. An (*abstract*) *simplicial complex* is a set Δ consisiting of subsets of V such that if $\sigma \in \Delta$, $\tau \subset \sigma$ then $\tau \in \Delta$. An element of Δ is a *face*. A *facet* is a face maximal with respect to set inclusion. An element of V is a *vertex*. The *dimension* of a face σ is $\dim \sigma = |\sigma| - 1$. The *dimension* of a simplicial complex Δ is $\max_{\sigma \in \Delta} \dim \sigma$. A simplicial complex is *pure* if all facets have the same dimension. A *ridge* of a pure simplicial complex is a face having dimension $\dim \Delta - 1$. A pure simplicial complex is a *pseudomanifold* if any ridge is included in at most two facets. If not, it is a *nonpseudomanifold*. A *boundary ridge* is a ridge contained in only one facet, and a facet containing a boundary ridge is a *boundary facet*. A d-dimensional simplicial complex, pseudomanifold, etc. will be denoted d-simplicial complex, d-pseudomanifold, etc. Two simplicial complexes which become identical by relabeling the vertices are called *isomorphic*, and are regarded as the same.

A *partial shelling* of a pure d-simplicial complex Δ is a sequence $F_1, \ldots, F_\ell$ of a subset of facets satisfying

$$\overline{F_i} \cap \left(\bigcup_{j=1}^{i-1} \overline{F_j} \right) \quad \text{is a pure } (d-1)\text{-simplicial complex} \quad (1 < i \le \ell), \qquad (*)$$

where $\overline{\sigma} = \{\tau \in \Delta : \tau \subset \sigma\}$. A *shelling* is a partial shelling consisting of all of the facets of Δ. A pure simplicial complex is *shellable* if it has a shelling. A partial shelling is *extendable* if there exists a shelling beginning from it. A maximal not extendable partial shelling is called *stuck*. A simplicial complex is *extendably shellable* if any partial shelling is extendable. In other words, extendable shellability means that we can find a shelling by adding facets in a greedy manner.

53

The *link* of a face $\sigma \in \Delta$ is $\text{link}_\Delta(\sigma) = \{\tau \in \Delta : \sigma \cup \tau \in \Delta, \sigma \cap \tau = \emptyset\}$. The *deletion* of a face $\sigma \in \Delta$ is $\text{del}_\Delta(\sigma) = \{\tau \in \Delta : \sigma \cap \tau = \emptyset\}$. A pure simplicial complex Δ is *vertex decomposable* if it has only one facet, or if it has a vertex i with both $\text{link}_\Delta(\{i\})$ and $\text{del}_\Delta(\{i\})$ vertex decomposable. A vertex decomposable simplicial complex is shellable.

We are interested in the case of dimension two. When a 2-simplicial complex has a 2-dimensional ball (resp. 2-dimensional sphere) as its realization, we simply call it a 2-*ball* (resp. 2-*sphere*). For the top dimensional element h_3 of the h-vector (or the reduced Euler characteristic), we have

$$h_3 = \#\text{facets} - \#\text{ridges (or edges)} + \#\text{vertices} - 1$$

(see, for example, [106, Chapter 8]).

For a 1-simplicial complex, shellability, extendable shellability, vertex decomposability, and connectivity are equivalent. This kind of simple situation holds until the case of 2-pseudomanifolds:

Theorem 5.4 ([26]). *For a 2-pseudomanifold, shellability, extendable shellability, vertex decomposability, and being a 2-ball or a 2-sphere are equivalent.*

5.3 Shellable but not extendably shellable simplicial complexes

5.3.1 Examples

We first give shellable but not extendably shellable 2-simplicial complexes found using the enumeration technique in Section 5.5. They include two known examples. Another larger known example V7F13 and two smaller examples V7F12, V7F11 made reversing the operation in Proposition 5.10 are also listed.

Example 5.5. *The following is a list of shellable but not extendably shellable 2-simplicial complexes. The list covers all such examples with less than 6 vertices, 6 vertices and at most 10 facets, or less than 9 facets, up to isomorphism. (Such examples do not exist for less than 6 vertices or less than 9 facets.) For the labeling, for example, V6F9-1 indicates the 1st example with 6 vertices and 9 facets. The 2-simplicial complexes are given as lists of facets, and boundary facets are printed in bold font. After the facets, are given the boundary ridges and all of the stuck partial shellings (unsorted, as sets) of the examples.*

V6F9-1	$124, \mathbf{126}, 134, \mathbf{135}, 245, 256, 346, 356, 456$
	boundary ridges : $15, 16$
	stuck partial shelling : $\{124, \mathbf{126}, 134, \mathbf{135}\}$
V6F9-2	$123, \mathbf{126}, \mathbf{135}, 234, 245, 256, 346, 356, 456$
	boundary ridges : $15, 16$
	stuck partial shelling : $\{123, \mathbf{126}, \mathbf{135}, 234\}$
V6F10-1 [92]	$\mathbf{123}, 124, \mathbf{126}, 134, \mathbf{135}, 245, 256, 346, 356, 456$
	boundary ridges : $15, 16, 23$
	stuck partial shelling : $\{\mathbf{123}, 124, \mathbf{126}, 134, \mathbf{135}\}$

|	
V6F10-2	$124, \mathbf{126}, 134, \mathbf{135}, \mathbf{236}, 245, 256, 346, 356, 456$
	boundary ridges : $15, 16, 23$
	stuck partial shelling : $\{124, \mathbf{126}, 134, \mathbf{135}\}$
V6F10-3	$123, \mathbf{126}, \mathbf{134}, \mathbf{135}, 234, 245, 256, 346, 356, 456$
	boundary ridges : $14, 15, 16$
	stuck partial shelling : $\{123, \mathbf{126}, \mathbf{134}, \mathbf{135}, 234\}$
V6F10-4	$123, 126, \mathbf{135}, \mathbf{146}, 234, 245, 256, 346, 356, 456$
	boundary ridges : $14, 15,$
	stuck partial shellings : $\{123, 126, \mathbf{135}, 234\},$
	$\{123, 126, \mathbf{135}, \mathbf{146}\}$
V6F10-5	$124, \mathbf{126}, 134, \mathbf{135}, \mathbf{234}, 245, 256, 346, 356, 456$
	boundary ridges : $15, 16, 23$
	stuck partial shelling : $\{124, \mathbf{126}, 134, \mathbf{135}, \mathbf{234}\}$
V6F11-1	$124, \mathbf{126}, 134, \mathbf{135}, 235, 236, 245, 256, 346, 356, 456$
	boundary ridges : $15, 16$
	stuck partial shelling : $\{124, \mathbf{126}, 134, \mathbf{135}\}$
V6F11-2	$123, 124, \mathbf{126}, 134, \mathbf{135}, 234, 245, 256, 346, 356, 456$
	boundary ridges : $15, 16$
	stuck partial shelling : $\{123, 124, \mathbf{126}, 134, \mathbf{135}, 234\}$
V6F11-3 [12, Exercise 7.37]	$123, 126, 135, 145, 146, 234, 245, 256, 346, 356, 456$
	boundary ridges : $\emptyset$
	stuck partial shelling : $\{123, 126, 135, 234\}$
V7F11	$a = 125, b = 126, c = 127, \boldsymbol{e} = \mathbf{145}, f = 167, h = 235,$
	$i = 236, \boldsymbol{j} = \mathbf{247}, k = 356, l = 457, m = 567$
	boundary ridges : $14, 24$
	stuck partial shelling : $\{\boldsymbol{e}, \boldsymbol{j}, k, l, m\}$
V7F12	$a = 125, b = 126, c = 127, \boldsymbol{e} = \mathbf{145}, f = 167, \boldsymbol{g} = \mathbf{234},$
	$h = 235, i = 236, j = 247, k = 356, l = 457, m = 567$
	boundary ridges : $14, 34$
	stuck partial shellings : $\{\boldsymbol{e}, \boldsymbol{g}, i, j, l\}, \{\boldsymbol{e}, \boldsymbol{g}, j, l, m\},$
	$\{\boldsymbol{e}, j, k, l, m\}$
V7F13 [51, Section 5.3]	$a = 125, b = 126, c = 127, \boldsymbol{d} = \mathbf{134}, e = 145, f = 167,$
	$g = 234, h = 235, i = 236, j = 247, k = 356, l = 457,$
	$m = 567$
	boundary ridge : 13
	stuck partial shellings : $\{a, b, \boldsymbol{d}, e, l\}, \{a, \boldsymbol{d}, e, l, m\},$
	$\{e, j, k, l, m\}, \{a, b, c, \boldsymbol{d}, e, f\}, \{\boldsymbol{d}, e, g, i, j, l\},$
	$\{\boldsymbol{d}, e, g, j, l, m\}, \{\boldsymbol{d}, g, h, i, j, k\}, \{\boldsymbol{d}, g, h, i, k, m\}$

Checking that these examples are shellable but not extendably shellable was also done using a

computer. However, for examples V6F9-1, 2, V6F10-1, 3, 4, 5, V7F11, V7F12 or V7F13, Lemma 5.6 below gives a proof of not being extendably shellable. This observation can be found, for example, in [97, Section III.2].

Lemma 5.6. *Let Δ be a shellable 2-simplicial complex with $h_3 = 0$. Then, the final facet in any of its shelling is a boundary facet. If there exists a proper partial shelling including all of the boundary facets, it does not extend to a shelling of Δ, and Δ is not extendably shellable.*

As can be observed from the examples, stuck partial shellings not including all of the boundary facets also exist.

Remark 5.7. *Topological drawings of V6F9-1, 2 are shown below. The boundary ridges are drawn in bold lines. The two examples differ only in the way the quadrilateral 1243 is triangulated. In V6F9-1 it is triangulated 124, 134, whereas in V6F9-2 it is triangulated 123, 234.*

V6F9-1   V6F9-2
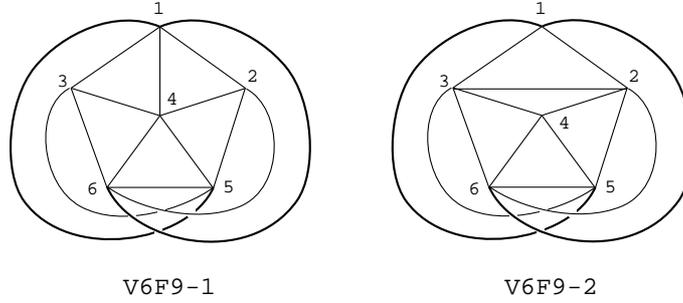
Remark 5.8. *All examples except V6F11-3 in Example 5.5 can be realized as geometric simplicial complexes without self intersection in three dimensional space. However, V6F11-3 cannot, because the subcomplex made by removing the facet 456 is the two dimensional projective space [12, Exercise 7.37].*

Remark 5.9. *Diagonal flips do not necessarily preserve the property shellable but not extendably shellable. For example, the 2-simplicial complex with facets 124, **126**, 134, **137**, 245, 256, 346, 356, **357**, 456, made by stellar subdivision of edge 15 in V6F9-1, is shellable but not extendably shellable. However, if we flip edge 26 to 15, removing facets 126, 256, and adding facets 125, 156 instead, the new 2-simplicial complex becomes shellable and extendably shellable.*

5.3.2 Relations

The following proposition gives a way to enlarge a shellable but not extendably shellable example, keeping a stuck partial shelling.

Proposition 5.10. *Let Δ be a shellable but not extendably shellable pure d-simplicial complex with $F_1, \ldots, F_i$ a stuck partial shelling. Take $\sigma \notin \Delta$, $\dim \sigma = d$ with $\overline{\sigma} \cap \Delta$ being a pure $(d-1)$-simplicial complex.*

(i) *If $\overline{\sigma} \cap \left(\bigcup_{j=1}^{i} \overline{F_j} \right)$ is not a pure $(d-1)$-simplicial complex, then $\Delta \cup \overline{\sigma}$ is shellable but not extendably shellable with $F_1, \ldots, F_i$ a stuck partial shelling.*

56

(ii) If $\overline{\sigma} \cap \left(\bigcup_{j=1}^{i} \overline{F_j} \right)$ is a pure $(d-1)$-simplicial complex and $\left(\overline{\sigma} \setminus \left(\bigcup_{j=1}^{i} \overline{F_j} \right) \right) \cap \Delta = \emptyset$ (which is equivalent for the τ satisfying $\left(\overline{\sigma} \setminus \left(\bigcup_{j=1}^{i} \overline{F_j} \right) \right) = \{\eta : \tau \subset \eta \subset \sigma\}$ being $\tau \notin \Delta$), then $\Delta \cup \overline{\sigma}$ is shellable but not extendably shellable with $F_1, \ldots, F_i, \sigma$ a stuck partial shelling.

Remark 5.11. *The operations in Proposition 5.10 defines relations between shellable but not extendably shellable examples. The ten examples V6F9-1, 2, V6F10-1, ..., 5, V6F11-1, ..., 3 are related by these operations as in the figure below.*
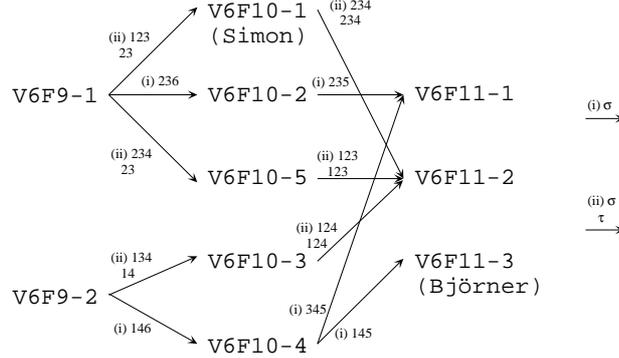
Remark 5.12. *If the vetrices of σ belong to Δ, and Δ includes all of the d-subsets (i.e. possible ridges) or one less than that, we do not have to check the condition "$\overline{\sigma} \cap \Delta$ being a pure $(d-1)$-simplicial complex" in Proposition 5.10. This is the case for the operations among examples V6F9-1, 2, V6F10-1, ..., 5, V6F11-1, ..., 3 in Remark 5.11.*

Another relation between the examples to consider is the set inclusion. We show some properties of minimal examples with respect to this relation.

A *homology facet* in a shelling is a facet with any of its proper subface included in some preceding facet in the shelling. If σ is a homology facet in some shelling of a simplicial complex Δ, by simply removing σ, a shelling of $\Delta \setminus \{\sigma\}$ can be made. In a shelling of a 2-simplicial complex, each homology facet contributes one to h_3.

Lemma 5.13. *Among the shellable but not extendably shellable 2-simplicial complexes, let Δ be a minimal one with respect to set inclusion. Then any proper partial shelling of Δ is extendably shellable. Thus any stuck partial shelling is extendably shellable. Furthermore, stuck partial shellings of Δ do not contain 2-spheres as subcomplexes.*

Proof. Straightforward. □

Proposition 5.14. *Among the shellable but not extendably shellable 2-simplicial complexes, let Δ be a minimal one with respect to set inclusion. Then Δ does not contain 2-spheres as subcomplexes.*

Proof. Straightforward. □

Remark that V6F9-1, 2, V7F11 are minimal with respect to set inclusion. Other interesting questions to consider might be (1) if minimal examples have $h_3 = 0$ (i.e. do not contain "homology 2-spheres"), (2) if minimal examples have the least number of facets for fixed number of vertices, or (3) if stuck partial shellings of such examples contain all of the boundary facets. Dealing with the relations by the operations in Proposition 5.10 is another interseting subject.

5.4 Shellable but not vertex decomposable simplicial complexes

We first give shellable but not vertex decomposable 2-simplicial complexes found using the enumeration technique in Section 5.5. They include one known example. Another larger known example `V7F13` is also listed.

Example 5.15. *The following is a list of shellable but not vertex decomposable 2-simplicial complexes. The list covers all such examples with less than 6 vertices, 6 vertices and at most 10 facets, or less than 9 facets, up to isomorphism. (Such examples do not exist for less than 6 vertices or less than 9 facets.) The 2-simplicial complexes are given as lists of facets, and boundary facets are printed in bold font. After the facets, are given the boundary ridges. Examples V6F10-6, 7 are not vertex decomposable but extendably shellable.*

`V6F10-1` [92]	*see Example 5.5*
`V6F10-6`	$\mathbf{123}, 124, \mathbf{125}, 134, \mathbf{136}, 245, \mathbf{256}, 346, \mathbf{356}, 456$
	boundary ridges : $15, 16, 23, 26, 35$
`V6F10-7`	$123, 125, \mathbf{126}, 134, 145, \mathbf{234}, 256, 346, \mathbf{356}, 456$
	boundary ridges : $16, 24, 35$
`V7F13` [51, Section 5.3]	*see Example 5.5*

Checking that these examples are shellable but not vertex decomposable was also done using a computer.

Extendable shellability and vertex decomposability are both properties stronger than shellability. Vertex decomposable but not extendably shellable simplicial complexes have been known (`V6F11-3` [12, Exercise 7.37], for example). On the other hand, examples `V6F10-6, 7` show the existence of extendably shellable but not vertex decomposable ones. Thus we know there are no implication between these two properties.

Corollary 5.16. *Neither extendable shellability nor vertex decomposability implies the other.*

Remark 5.17. *All examples in Example 5.15 can be realized as geometric simplicial complexes without self intersection in three dimensional space.*

Remark 5.18. *Diagonal flips do not necessarily preserve the property shellable but not vertex decomposable. For example, the 2-simplicial complex with facets* $\mathbf{123}, 124, \mathbf{126}, 134, 135, \mathbf{157}, 245, 256, 346, 356, 456$, *made by adding a 2-simplex 157 to the boundary edge 15 in* `V6F10-1`, *is shellable but not vertex decomposable. However, if we flip edge 15 to 37, removing facets 135, 157, and adding facets 137, 357 instead, the new 2-simplicial complex becomes shellable and vertex decomposable.*

5.5 Enumeration of shellable nonpseudomanifolds

We call the 2-simplicial complex with five vertices $1, \ldots, 5$ and three facets 123, 124, 125 the *initial simplicial complex*, and denote it by Δ_{initial}. This is the minimal 2-nonpseudomanifold. For a 2-simplicial complex, we also call a subcomplex isomorphic to Δ_{initial} an *initial simplicial complex*.

Proposition 5.19. *For any shellable 2-nonpseudomanifold Δ, there exists a shelling beginning from one of its initial simplicial complexes.*

Proof. Straightforward. □

Algorithm 5.20. *Begin from Δ_{initial}. Add facets one by one in a shelling manner (i.e. satisfying $(*)$ in Section 5.2). The shellable nonpseudomanifolds with v vertices and f facets are made from those with v or $v-1$ vertices and $f-1$ facets.*

Theorem 5.21. *Algorithm 5.20 enumerates shellable 2-simplicial complexes which are not pseudomanifolds.*

Proof. Proposition 5.19. □

During the enumeration, for each size of vertices and facets, we only want to output one simplicial complex among the isomorphic ones. This can be done using the following lemma.

Lemma 5.22. *We can find a canonical (e.g. lexicographically minimal) labeling with respect to isomorphism of a 2-simplicial complex with v vertices and f facets in $O(v!vf)$ time.*

Proof. Consider the vertex facet incidence matrix. Make all copies for the $v!$ different vertex labelings. Remark that $v \leq f+2$ for the examples we are interested in. Use radix sort. □

Finally, the numbers of isomorphism classes of shellable nonpseudomanifolds we enumerated are shown in Table 5.1.

# of vertices	# of facets																	
	3	4	5	6	7	8	9	10	11	12	13	14	15	16	17	18	19	20
5	1	1	3	4	4	2	1	1										
6		2	8	23	51	100	170	254	269	233	157	93	43	21	7	3	1	1
7			8	42	167	535	1628	4722	⋯									
8				27	217	1114	⋯											
9					109	1106	⋯											
10						447	⋯											

Table 5.1: The number of isomorphism classes of shellable two dimensional nonpseudomanifolds with specified numbers of vertices and facets.

5.6 Conclusion

We showed small examples (including minimal ones) showing difference between shellability, extendable shellability, and vertex decomposability. Shellable but not extendably shellable ones were smaller than those previously known. Shellable but not vertex decomposable ones included extendably shellable ones, which shows that neither extendable shellability nor vertex decomposability implies the other. We also discussed on topological properties of minimal examples, and on the

enumeration of shellable nonpseudomanifolds. This is an important starting step, but still we need to *understand* what is happening. Nice questions to begin by might be the following:

- Are there "minimal examples" in the sense that we can construct all other examples on basis of those? What (topological) properties do "minimal examples" have? How about a "forbidden minor approach"?

Another problem, which was the motivation of this study, but still unsolved is the following:

- What is the computational complexity of deciding shellability, extendable shellability, or vertex decomposability of a given (two dimensional) simplicial complex? Are they NP-complete?

Chapter 6

Computational approaches for triangulations

Summaries of our results and their possible applications were discussed in Chapter 1. Evaluations of our results and indications on future studies appeared in the concluding sections of Chapters 2 to 5. We avoid repeating them, but discuss here on an approach in this study: using computers to generate and test examples.

Using computers for triangulations. Recently, there have been some works using computers for solving combinatorial geometric problems of triangulations (as those problems treated in this thesis) [31] [67] [72] [101] [102] [105]. (Of course, there have been many works using triangulations in computational geometry.) We exploited several of these previous results and also used new algorithms. Extensive use of computer for combinatorial geometric aspects of triangulations is a peculiarity of this work.

Generating and testing examples. We have been interested in differences between classes of objects or properties, such as, dissections and triangulations, regular triangulations and nonregular triangulations, shellings and geometric shellings, and shellability, extendable shellability and vertex decomposability. A large portion of this thesis was giving concrete examples showing these differences.

These examples were sometimes generated and almost always tested using a computer. Computations using computers do not produce meaningful examples automatically, but they do help. On the other hand, computers are indispensable when checking examples.

Algorithmic approaches. Some of the algorithms we used for generating or testing triangulations are based on other established techniques such as integer programming or linear programming. Main programs used in this study are listed with the techniques behind them:

Chapter 2:

- enumerating triangulations: [105] by enumeration of maximal independent sets, [82],

- enumerating dissections: [105] by enumeration of maximal independent sets,

- finding minimal/maximal triangulations: [31] [101] [102] by integer programming,

Chapter 3:

- deciding regularity of a triangulation: by linear programming,

- computing the solutions of a dual problem: convex hull computations [3] [42] [22],

Chapter 5:

- enumerating shellable 2-nonpseudomanifolds,

- enumerating shellings/deciding shellability,

- deciding vertex decomposability.

The approach using a computer benefits when the problem is beyond our initial intuition, but in reach of computer power. The works in this thesis show benefits thus obtained. Assembling programs and examples on triangualations, as in the POLYMAKE [58] project for polytopes, must lead to further results in this direction.

Appendix A

More generalizations of triangulations

Two more generalization of triangulations not given in chapter 1 are discussed. Each section introduces a generalization of triangulations and discuss their applications and properties of interest, though restricting mainly to those subjects relevant to our results. Our results might give suggestions on designing algorithms for these applications.

A.1 Pseudo-triangulations

A.1.1 Definitions and examples

Pseudo-triangulations (or geodesic triangulations) (see [79]) are generalizations of triangulations in dimension two. The given polygon is partitioned into pseudo-triangles. A *pseudo-triangle* is a polygon with three vertices having internal angles less than π and the other vertices at least π. A triangle is a pseudo-triangle, and a triangulation is a pseudo-triangulation.

Definition A.1. *Given points $p_1, \ldots, p_n \in \mathbb{R}^2$ and a (possibly nonconvex) polygon including these points and with vertices among the points, a set of pseudo-triangles with vertices among these points is a* pseudo-triangulation *if (1) any pair of pseudo-triangles have no interior point in common, (2) the union of the pseudo-triangles is equal to the polygon, and (3) any point appears as a vertex of some pseudo-triangle.*
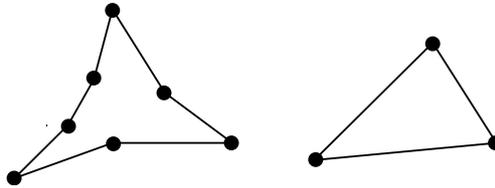
Figure A.1: Pseudo-triangles.
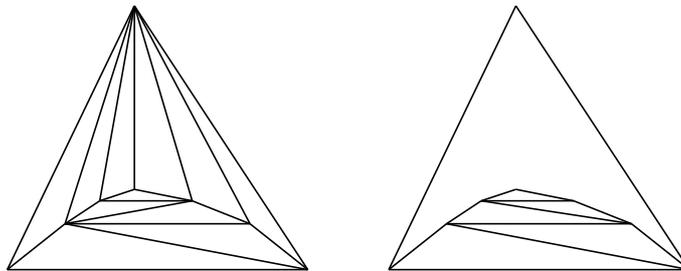
Figure A.2: A triangulation and a pseudo-triangulation

A.1.2 Applications

Kinetic data structure

Pseudo-triangulations form a superclass of triangulations. They have been used in ray shooting [21] [47] or visibility [80] [78]. Recently, they have been applied to kinetic data structure for collision detection [1] [64] [65] [98].

A.1.3 Properties and questions

Size and complexity

By the *size* of a pseudo-triangulation, we mean the number of pseudo-triangles in it. For any point configuration of n points in general position (i.e. no three points on a line) and a simple polygon (i.e. without holes) including the points and with vertices among the points, the pseudo-triangulation has size at least $n - 2$. There always exist pseudo-triangulations of this size $n - 2$, and we call them *minimal*.

The *degree* of a pseudo-triangulation is the largest number of edges sharing a vertex. Among the minimal pseudo-triangles, one of the next objective becomes to find one with minimal degree. For any point configuration in general position and a convex polygon, differently from the case of triangulations, the degree of (minimal) pseudo-triangulations can be bounded by a constant six [61]. This *locality* property is needed when applied to kinetic data structure.

A.1.4 Our contribution

We give a point configuration in general position and a convex polygon, any of their minimal pseudo-triangulations has degree at least five [61].

A.2 Oriented matroid triangulations

A.2.1 Definitions

Oriented matroids are combinatorial abstractions of point configurations (see [15] for the terminology in this section). Any point configuration defines a (realizable) oriented matroid. In the oriented matroid level, we forget the coordinates of the points, but still keep some information on the original point configuration, namely the affine dependencies. Triangulations have been extended to this abstract level:

Definition A.2 ([10]). *Let $\mathcal{M}$ be an acyclic oriented matroid of rank $d + 1$ on a set V. A non-empty collection Δ of bases of $\mathcal{M}$ is a triangulation of $\mathcal{M}$ if it satisfies*

- *for every single element extension $\mathcal{M} \cup p$ of $\mathcal{M}$ and every $\sigma, \tau \in \Delta$, $p \in \mathrm{conv}_{\mathcal{M} \cup p}(\sigma) \cap \mathrm{conv}_{\mathcal{M} \cup p}(\tau)$ implies $p \in \mathrm{conv}_{\mathcal{M} \cup p}(\sigma \cap \tau)$;*

- *if $\sigma, \tau \in \Delta$, then $\sigma \cap \tau$ is a common face of the two restrictions $\mathcal{M}(\sigma)$ and $\mathcal{M}(\tau)$;*

- *if $\sigma \in \Delta$, then each facet of $\mathcal{M}(\sigma)$ is either a facet of $\mathcal{M}$ or is contained in precisely two cells of Δ.*

A.2.2 Backgrounds

The study of triangulations of oriented matroids started from [10]. Recently, extensive study especially on lifting triangulations has been done in [87].

A.2.3 Properties and questions

Regularity

As discussed in Section 1.1.3, regularity is an important issue for triangulations (with coordinates). In oriented matroid triangulations, lifting triangulation is a similar but different subject. The oriented matroid counterpart of regular triangulations must be important but is not yet well understood.

A.2.4 Our contribution

We study what regularity means for oriented matroid triangulations. For this aim, we introduce the idea of "circuits of circuits". We also study how strong information oriented matroid triangulations have, and use them for classifying point configurations [60].

References

[1] PANKAJ K. AGARWAL, JULIEN BASCH, LEONIDAS J. GUIBAS, JOHN HERSHBERGER, LI ZHANG, Deformable free space tiling for kinetic collision detection, in: Proc. 4th Workshop Algorithmic Found. Robot., 2000.

[2] NINA AMENTA, GÜNTER M.ZIEGLER, Deformed products and maximal shadows of polytopes, *Contemporary Mathematics* **223** (1999) 57–90.

[3] DAVID AVIS, lrs, a convex hull program, ftp://mutt.cs.mcgill.ca/pub/C

[4] ALEXANDER BARVINOK, JAMES E. POMMERSHEIM, An algorithmic theory of lattice points in polyhedra, in: New Perspectives in Algebraic Combinatorics, MSRI book series, **38** Cambridge University Press, Cambridge, 1999.

[5] ALEXANDER BELOW, ULRICH BREHM, JESÚS A. DE LOERA, JÜRGEN RICHTER-GEBERT, Minimal simplicial dissections and triangulations of convex 3-polytopes, *Discrete and Comp. Geom.* **24** (2000) 35–48.

[6] ALEXANDER BELOW, JESÚS A. DE LOERA, JÜRGEN RICHTER-GEBERT, Finding minimal triangulations of convex 3-polytopes is NP-hard, in: Proc. 11th Symp. Discrete Algorithms, 65–66, ACM, New York, 2000.

[7] LOUIS J. BILLERA, PAUL FILLIMAN, BERND STURMFELS, Constructions and complexity of secondary polytopes, *Adv. Math.* **83** (1990) 155–179.

[8] LOUIS J. BILLERA, CARL W. LEE, Sufficiency of McMullen's conditions for f-vectors of simplicial polytopes, *Bull. Amer. Math. Soc.* **2** (1980) 181–185.

[9] LOUIS J. BILLERA, CARL W. LEE, A proof of the sufficiency of McMullen's conditions for f-vectors of simplicial convex polytopes, *J. Combinatorial Theory, Ser. A* **31** (1981) 237–255.

[10] LOUIS J. BILLERA, BETH SPELLMAN MUNSON, Triangulations of oriented matroids and convex polytopes. *SIAM J. Algebraic Discrete Methods* **5** (1984) 515–525.

[11] LOUIS J. BILLERA, J. SCOTT PROVAN, A decomposition property for simplicial complexes and its relation to diameters and shellings *Ann. New York Acad. Sci.* **319** (1979) 82–85.

[12] ANDERS BJÖRNER, The homology and shellability of matroids and geometric lattices, in: Matroid applications, pp.226–283, Encyclopedia Math. Appl., 40, Cambridge Univ. Press, Cambridge, 1992.

[13] ANDERS BJÖRNER, Topological methods, in: Handbook of combinatorics, pp.1819–1872, Elsevier, Amsterdam, 1995.

[14] ANDERS BJÖRNER, KIMMO ERIKSSON, Extendable shellability for rank 3 matroid complexes, *Discrete Math.* **132** (1994) 373–376.

[15] ANDERS BJÖRNER, MICHEL LAS VERGNAS, BERND STURMFELS, NEIL WHITE, GÜNTER ZIEGLER, Oriented matroids, 2nd ed., Encyclopedia of Mathematics and its Applications **46**, Cambridge University Press, Cambridge, 1999.

[16] BÉLA BOLLOBÁS, Modern graph theory, Springer-Verlag, New York, 1998.

[17] GLEN E. BREDON, *Topology and geometry*, Springer-Verlag, New York, 1993.

[18] HEINZ BRUGGESSER, PETER MANI, Shellable decompositions of cells and spheres, *Math. Scand.* **29** (1971) 197–205.

[19] WINFRIED BRUNS, JOSEPH GUBELADZE, NGÔ VIÊT TRUNG Normal polytopes, triangulations and Koszul algebras *J. Reine Angew. Math.* **485** (1997) 123–160.

[20] CG IMPACT TASK FORCE, Application challenges to computational geometry, *Contemporary Mathematics* **223** (1999) 407–463.

[21] BERND CHAZELLE, HERBERT EDELSBRUNNER, M. GRIGNI, LEONIDAS J. GUIBAS, JOHN HERSHBERGER, MICHA SHARIR, JACK SNOEYINK, Ray shooting in polygons using geodesic triangulations. *Algorithmica* **12** (1994) 54–68.

[22] THOMAS CHRISTOF, PORTA, a convex hull program, ftp://elib.zib-berlin.de/pub/mathprog/polyth/porta

[23] HAROLD SCOTT MACDONALD COXETER, Regular Polytopes, Dover Publications, New York, 1973.

[24] HALLARD T. CROFT, KENNETH J. FALCONER, RICHARD K. GUY, Unsolved problems in geometry, Springer-Verlag, New York, 1994.

[25] GOPAL DANARAJ, VICTOR KLEE, Which spheres are shellable?, *Ann. Discrete Math.* **2** (1978) 33–52.

[26] GOPAL DANARAJ, VICTOR KLEE, A representation of 2-dimensional pseudomanifolds and its use in the design of a linear-time shelling algorithm, *Ann. Discrete Math.* **2** (1978) 53–63.

[27] G.B. DANTZIG, A.J. HOFFMAN, T.C. HU, Triangulations (tilings) and certain block triangular matrices, *Mathematical Programming* **31** (1985) 1–14.

[28] HUBERT DE FRAYSSEIX, PATRICE OSSONA DE MENDEZ, On topological aspects of orientations, *Discrete Math.* to appear.

[29] HUBERT DE FRAYSSEIX, JÁNOS PACH, RICHARD POLLACK, How to draw a planar graph on a grid, *Combinatorica* **10** (1990) 41–51.

68

[30] CECIL JOSE A. DELFINADO, HERBERT EDELSBRUNNER, An incremental algorithm for Betti numbers of simplicial complexes on the 3-sphere, Grid generation, finite elements, and geometric design. *Comput. Aided Geom. Design* **12** (1995) 771–784.

[31] JESÚS A. DE LOERA, SERKAN HOŞTEN, FRANCISCO SANTOS, BERND STURMFELS, The polytope of all triangulations of a point configuration, *Doc. Math.*, **1** (1996) 103–119.

[32] TAMAL K. DEY, HERBERT EDELSBRUNNER, SUMANTA GUHA, Computational topology, *Contemporary Mathematics* **223** (1999) 109–143.

[33] JESUS A. DE LOERA, FRANCISCO SANTOS, FUMIHIKO TAKEUCHI, Extremal properties for dissections of convex 3-polytopes, *SIAM J. Discrete Math.*, to appear.

[34] ANDREAS DRESS, A new algebraic criterion for shellability, *Beiträge Algebra Geom.* **34** (1993) 45–55.

[35] HERBERT EDELSBRUNNER, *Algorithms in combinatorial geometry*, Springer-Verlag, Berlin, 1987.

[36] HERBERT EDELSBRUNNER, An acyclicity theorem for cell complexes in d dimension, *Combinatorica*, **10** (1990) 251–260.

[37] HERBERT EDELSBRUNNER, MICHAEL FACELLO, JIE LIANG, On the definition and the construction of pockets in macromolecules, *Discrete Appl. Math.* **88** (1998) 83–102.

[38] HERBERT EDELSBRUNNER, ERNST PETER MÜCKE, Three-dimensional alpha shapes, ACM Trans. Graph., **13** (1994) 43–72.

[39] HERBERT EDELSBRUNNER, F.P. PREPARATA, D.B. WEST, Tetrahedrizing point sets in three dimensions, *J. Symbolic Comput.* **10** (1990) 335–347.

[40] GÜNTER EWALD, Combinatorial convexity and algebraic geometry, Springer-Verlag, New York, 1996.

[41] R.T. FIRLA, GÜNTER M. ZIEGLER, Hilbert bases, unimodular triangulations, and binary covers of rational polyhedral cones, *Discrete Comput. Geom.* **21** (1999) 205–216.

[42] KOMEI FUKUDA, cdd, a convex hull program, ftp://ifor13.ethz.ch/pub/fukuda/cdd

[43] BERND GÄRTNER, EMO WELZL, Linear programming—randomization and abstract frameworks. in: Proc. STACS '96, Lecture Notes in Comput. Sci. 1046, Springer, Berlin, 1996, 669–687.

[44] ISRAEL M. GELFAND, MIKHAIL M. KAPRANOV, ANDREI V. ZELEVINSKY, *Discriminants, resultants and multidimensional determinants*, Birkhäuser, Boston, 1994.

[45] ISRAEL M. GEL'FAND, ANDREI V. ZELEVINSKIĬ, MIKHAIL M. KAPRANOV, Newton polyhedra of principal A-determinants, *Soviet Math. Dokl.*, **40** (1990) 278–281.

[46] J.E. GOODMAN, J. O'ROURKE, EDS., Handbook of Discrete and Computational Geometry, CRC Press, Boca Raton, 1997, 271–290.

[47] MICHAEL T. GOODRICH, ROBERTO TAMASSIA, Dynamic ray shooting and shortest paths in planar subdivisions via balanced geodesic triangulations. *J. Algorithms* **23** (1997) 51–73.

[48] PETER GRITZMANN, VICTOR KLEE, On the complexity of some basic problems in computational convexity: II. Volume and mixed volumes. in: T. Bisztriczky et al. eds., Polytopes: Abstract, convex and computational, 373–466, Kluwer Academic Publishers, Netherlands, 1994.

[49] BRANKO GRÜNBAUM, Convex Polytopes, Interscience Publishers Wiley and Sons, London, 1967.

[50] BRANKO GRÜNBAUM, V. P. SREEDHARAN, An enumeration of simplicial 4-polytopes with 8 vertices, *J. Comb. Theory* **2** (1967) 437–465.

[51] MASAHIRO HACHIMORI, Combinatorics of constructible complexes, Ph.D. thesis, Univ. of Tokyo, Tokyo, 2000.

[52] MARK HAIMAN, A simple and relatively efficient triangulation of the n-cube, *Discrete Comput. Geom.* **6** (1991) 287–289.

[53] FRED HOLT, VICTOR KLEE, A proof of the strict monotone 4-step conjecture, *Contemporary Mathematics* **223** (1999) 201–216.

[54] BIRKETT HUBER, JÖRG RAMBAU, FRANCISCO SANTOS, The Cayley trick, lifting subdivisions and the Bohne-Dress theorem on zonotopal tilings, *J. Eur. Math. Soc.* **2** (2000) 179–198.

[55] ROBERT B. HUGHES, MICHAEL R. ANDERSON, Simplexity of the cube, *Discrete Math.* **158** (1996) 99–150.

[56] MARTIN ISENBERG, JACK SNOEYINK, Face Fixer: compressing polygon meshes with properties, in: Proc. SIGGRAPH 2000, 263–270.

[57] TAKAYUKI ISHIZEKI, FUMIHIKO TAKEUCHI, Geometric shellings of 3-polytopes, in: Proc. 11th Canadian conference on computational geometry, Vancouver, 1999, 132–135.

[58] MICHAEL JOSWIG, EWGENIJ GAWRILOW, POLYMAKE: A software package for polytopes, http://www.math.tu-berlin.de/diskregeom/polymake/doc/

[59] JEAN-MICHEL KANTOR, Triangulations of integral polytopes and Ehrhart polynomials, *Beiträge Algebra Geometrie* **39** (1998) 205–218.

[60] KENJI KASHIWABARA, FUMIHIKO TAKEUCHI, Oriented matroid triangulations: regularity and circuits of circuits, in preparation.

[61] LUTZ KETTNER, ANDREA MANTLER, JACK SNOEYINK, BETTINA SPECKMANN, FUMIHIKO TAKEUCHI, Bounded-degree pseudo-triangulations of points, manuscript.

[62] LUTZ KETTNER, JAREC ROSSIGNAC, JACK SNOEYINK A geometric basis for visualizing 4D data sets, manuscript.

[63] SIMON A. KING How to make a triangulation of S^3 polytopal, preprint.

[64] DAVID KIRKPATRICK, JACK SNOEYINK, BETTINA SPECKMANN, Kinetic collision detection for simple polygons in: Proc. 16th ACM Symp. Comp. Geom., 322–330, 2000.

[65] DAVID KIRKPATRICK, BETTINA SPECKMANN, Separation sensitive kinetic collision detection for simple polygons, in: Proc. Japan Conf. Disc. Comput. Geom. 2000, Springer-Verlag, to appear.

[66] VICTOR KLEE, DAVID W. WALKUP, The d-step conjecture for polyhedra of dimension $d < 6$, Acta Math. **117** (1967) 53–78.

[67] YOSHIAKI KYODA, KEIKO IMAI, FUMIHIKO TAKEUCHI, AKIRA TAJIMA, A branch-and-cut approach for minimum weight triangulation, in: Hon Wai Leong, Hiroshi Imai, eds., Proc. of 8th Annual International Symposium on Algorithms and Computation (ISAAC '97), Lecture Notes in Computer Science 1350, Springer-Verlag, Berlin, 384–393.

[68] JEFFREY C. LAGARIAS, GÜNTER M. ZIEGLER, Unimodular triangulations, manuscript, 1999.

[69] CARL W. LEE, Regular triangulations of convex polytopes, DIMACS Series in Discrete Mathematics and Theoretical Computer Science **4**, Amer. Math. Soc., 1991, 443–456.

[70] CARL W. LEE, Subdivisions and triangulations of polytopes, in: J.E. Goodman, J. O'Rourke, eds., Handbook of Discrete and Computational Geometry, CRC Press, Boca Raton, 1997, 271–290.

[71] PATRICK SCOTT MARA, Triangulations for the cube, J. Combinatorial Theory Ser. A **20** (1976) 170–177.

[72] TOMONARI MASADA, HIROSHI IMAI, KEIKO IMAI, Enumeration of regular triangulations, in: Proc. 12th Annual ACM Symposium on Computational Geometry, New York 1996, 224–233.

[73] PETER MCMULLEN, The maximum numbers of faces of a convex polytope, Mathematika, **17** (1970) 179–184.

[74] JAMES MIHALISIN, VICTOR KLEE, Convex and linear orientations of polytopal graphs. Discrete Comput. Geom. **24** (2000) 421–435.

[75] SONOKO MORIYAMA, Extendable shellability in dimension two, Bachelor thesis, Univ. of Tokyo, Tokyo, 2000.

[76] SONOKO MORIYAMA, FUMIHIKO TAKEUCHI, Incremental construction properties in dimension two—shellability, extendable shellability and vertex decomposability, in: Proc. 12th Canadian conference on computational geometry, Fredericton, 2000, 65–72.

[77] HIDEFUMI OHSUGI, TAKAYUKI HIBI, A normal $(0, 1)$-polytope none of whose regular triangulations is unimodular, *Discrete Comput. Geom.* **21** (1999) 201–204.

[78] MICHEL POCCHIOLA, GERT VEGTER, Topologically sweeping visibility complexes via pseudotriangulations. *Discrete Comput. Geom.* **16** (1996) 419–453.

[79] MICHEL POCCHIOLA, GERT VEGTER, Pseudo-triangulations: Theory and applications, in: Proc. 12th Symposium on Computational Geometry, 291–300, 1996.

[80] MICHEL POCCHIOLA, GERT VEGTER, Minimal tangent visibility graphs. *Comput. Geom.* **6** (1996) 303–314.

[81] J. SCOTT PROVAN, LOUIS J. BILLERA, Decompositions of simplicial complexes related to diameters of convex polyhedra, *Math. Oper. Res.* **5** (1980) 576–594.

[82] JÖRG RAMBAU, TOPCOM: a program for computing all triangulations of a point set, ZIB-Berlin, 1999. http://www.zib.de/rambau/TOPCOM.html

[83] JÜRGEN RICHTER-GEBERT Realization spaces of polytopes. Lecture notes in Mathematics **1643**, Springer-Verlag, 1996.

[84] B.L. ROTHSCHILD, E.G. STRAUS, On triangulations of the convex hull of n points, *Combinatorica* **5** (1985) 167–179.

[85] JIM RUPPERT, RAIMUND SEIDEL, On the difficulty of triangulating three-dimensional nonconvex polyhedra, *Discrete Comput. Geom.* **7** (1992) 227–253.

[86] FRANCISCO SANTOS, A point configuration whose space of triangulations is disconnected, *J. Amer. Math. Soc.*, **13** (2000) 611–637.

[87] FRANCISCO SANTOS, Triangulations of oriented matroids, *Memoirs Amer. Math. Soc.*, to appear. Available at
http://www.matesco.unican.es/~santos/Articulos/index.html

[88] ALEXANDER SCHRIJVER, Theory of linear and integer programming, John Wiley & Sons, Chichester, 1986.

[89] ANDRÁS SEBÖ, Hilbert bases, Carathéodory's theorem and combinatorial optimization, in: R. Kannan, W. Pulleyblank eds., Integer programming and combinatorial optimization, Math. Programming society, University of Waterloo Press, Waterloo 1990, 431–456.

[90] ANDRÁS SEBÖ, An introduction to empty lattice simplices, manuscript 2000. Available at
http://cosmos.imag.fr/DMD/OPTICOMB/Membres/sebo/sebo.html

[91] RAIMUND SEIDEL, Constructing higher dimensional convex hulls at logarithmic cost per face, in: Proc. 18th Annual ACM Symposium on Theory of Computing (STOC), pp.404–413, 1986.

[92] ROBERT SAMUEL SIMON, Combinatorial properties of "cleanness", *J. Algebra* **167** (1994) 361–388.

[93] ZEEV SMILANSKY, A non-geometric shelling of a 3-polytope, *Israel J. of Math.* **71** (1990) 29–32.

[94] WARREN D. SMITH A lower bound for the simplexity of the n-cube via hyperbolic volumes, *European J. Combin.* **21** (2000) 131–137.

[95] RICHARD P. STANLEY, The upper bound conjecture and Cohen-Macaulay rings, *Studies in Applied Math.* **54** (1975) 135–142.

[96] RICHARD P. STANLEY, The number of faces of a simplicial convex polytope, *Adv. Math.* **35** (1980) 236–238.

[97] RICHARD P. STANLEY, Combinatorics and commutative algebra, Birkhäuser, Boston, 2nd ed., 1996.

[98] ILEANA STREINU, A combinatorial approach to planar non-colliding robot arm motion planning, in: Proc. 41st Symp. Foundations of Computer Science, 443–453, 2000.

[99] BERND STURMFELS, Gröbner bases of toric varieties, *Tôhoku Math. J.*, **43** (1991) 249–261.

[100] BERND STURMFELS, *Gröbner bases and convex polytopes*, American Mathematical Society, Providence, RI, 1996.

[101] AKIRA TAJIMA, Optimality and integer programming formulations of triangulations in general dimension, in: K.-Y. Chwa, O.H. Ibarra eds., Proc. of 9th Annual International Symposium on Algorithms and Computation (ISAAC '98), Lecture Notes in Computer Science 1533, Springer-Verlag, Berlin, 377–386.

[102] AKIRA TAJIMA, Optimizing geometric triangulations by using integer programming, Ph.D. Thesis, Univ. of Tokyo, Tokyo, 2000. Available at
http://www-imai.is.s.u-tokyo.ac.jp/~akira/papers/dissertation.pdf

[103] FUMIHIKO TAKEUCHI, Nonregular triangulations, view graphs of triangulations, and linear programming duality, *Sūrikaisekikenkyūsho Kōkyūroku* **1175** (2000) 77–85.

[104] FUMIHIKO TAKEUCHI, Nonregular triangulations, view graphs of triangulations, and linear programming duality, in: Proc. Japan Conf. Disc. Comput. Geom. 2000, Springer-Verlag, to appear.

[105] FUMIHIKO TAKEUCHI, HIROSHI IMAI, Enumerating triangulations for products of two simplices and for arbitrary configurations of points, in: T. Jiang, D. T. Lee eds., Proc. of 3rd Annual International Conference on Computing and Combinatorics (COCOON '97), Lecture Notes in Computer Science 1276, Springer-Verlag, Berlin, 470–481.

[106] GÜNTER M. ZIEGLER, Lectures on polytopes, Springer-Verlag, New York, 1995.

[107] GÜNTER M. ZIEGLER, Shelling polyhedral 3-balls and 4-polytopes, *Discrete Comput. Geom.* **19** (1998) 159–174.

Index